Circulation Research

ORIGINAL RESEARCH

RNF149 Destabilizes IFNGR1 in Macrophages to Favor Postinfarction Cardiac Repair

Chun-Kai Huang, Zhiyong Chen, Zhongxing Zhou, Shuaijie Chen, Longqing Chen, Liliang Li, Tao Li, Xiaoxiang Yan, Dajun Chai

BACKGROUND: Macrophage-driven inflammation critically involves in cardiac injury and repair following myocardial infarction (MI). However, the intrinsic mechanisms that halt the immune response of macrophages, which is critical to preserve homeostasis and effective infarct repair, remain to be fully defined. Here, we aimed to determine the ubiquitination-mediated regulatory effects on averting exaggerated inflammatory responses in cardiac macrophages.

METHODS: We used transcriptome analysis of mouse cardiac macrophages and bone marrow–derived macrophages to identify the E3 ubiquitin ligase RNF149 (ring finger protein 149) as a modulator of macrophage response to MI. Employing loss-of-function methodologies, bone marrow transplantation approaches, and adenovirus-mediated RNF149 overexpression in macrophages, we elucidated the functional role of RNF149 in MI. We explored the underlying mechanisms through flow cytometry, transcriptome analysis, immunoprecipitation/mass spectrometry analysis, and functional experiments. RNF149 expression was measured in the cardiac tissues of patients with acute MI and healthy controls.

RESULTS: RNF149 was highly expressed in murine and human cardiac macrophages at the early phase of MI. Knockout of RNF149, transplantation of *Rnf149*$^{-/-}$ bone marrow, and bone marrow macrophage–specific RNF149-knockdown markedly exacerbated cardiac dysfunction in murine MI models. Conversely, overexpression of RNF149 in macrophages attenuated the ischemia-induced decline in cardiac contractile function. RNF149 deletion increased infiltration of proinflammatory monocytes/macrophages, accompanied by a hastened decline in reparative subsets, leading to aggravation of myocardial apoptosis and impairment of infarct healing. Our data revealed that RNF149 in infiltrated macrophages restricted inflammation by promoting ubiquitylation-dependent proteasomal degradation of IFNGR1 (interferon gamma receptor 1). Loss of IFNGR1 rescued deleterious effects of RNF149 deficiency on MI. We further demonstrated that STAT1 (signal transducer and activator of transcription 1) activation induced *Rnf149* transcription, which, in turn, destabilized the IFNGR1 protein to counteract type-II IFN (interferon) signaling, creating a feedback control mechanism to fine-tune macrophage-driven inflammation.

CONCLUSIONS: These findings highlight the significance of RNF149 as a molecular brake on macrophage response to MI and uncover a macrophage-intrinsic posttranslational mechanism essential for maintaining immune homeostasis and facilitating cardiac repair following MI.

GRAPHIC ABSTRACT: A graphic abstract is available for this article.

Key Words: cardiovascular diseases ■ inflammation ■ macrophages ■ myocardial infarction ■ ubiquitination

Meet the First Author, see p 473

Myocardial infarction (MI) remains the most prevalent cause of morbidity and mortality among all cardiovascular diseases.[1] In clinical practice, limiting infarction extent is conventionally achieved through timely coronary reperfusion. Nevertheless, a portion of patients with MI still develop adverse cardiac

Correspondence to: Chun-Kai Huang, MD, PhD, Cardiovascular Department, First Affiliated Hospital, Fujian Medical University, 20 Chazhong Rd, Fuzhou, Fujian 350005, PR China, Email chun-kai-huang@outlook.com; Xiaoxiang Yan, MD, PhD, Department of Cardiovascular Medicine, Ruijin Hospital, Shanghai Jiao Tong University School of Medicine, 197 Ruijin 2nd Rd, Shanghai 200025, PR China, Email cardexyanxx@hotmail.com; or Dajun Chai, MD, PhD, Cardiovascular Department, First Affiliated Hospital, Fujian Medical University, 20 Chazhong Rd, Fuzhou, Fujian 350005, PR China, Email dajunchai-fy@fjmu.edu.cn
Supplemental Material is available at https://www.ahajournals.org/doi/suppl/10.1161/CIRCRESAHA.123.324023.
For Sources of Funding and Disclosures, see page 535.

Circulation Research is available at www.ahajournals.org/journal/res

Novelty and Significance

What Is Known?

- Macrophage-mediated inflammation plays a pivotal role in the ischemic injury, repair, and remodeling of the infarcted heart.
- E3 ubiquitin ligases modulate the degradation or functional activities of proteins implicated in innate immunity, thereby acting as safeguards against excessive immune responses.

What New Information Does This Article Contribute?

- The E3 ligase RNF149 (ring finger protein 149) is highly expressed in murine and human cardiac macrophages during the early phase of myocardial infarction (MI).
- RNF149 deletion increased infiltration of proinflammatory monocytes/macrophages, accompanied by a hastened decline in reparative subsets, leading to impairment of infarct healing and aggravation of cardiac dysfunction in a mouse MI model.
- STAT1 (signal transducer and activator of transcription 1)-mediated transcription of *Rnf149* induces the ubiquitylation-dependent proteasomal degradation of IFNGR1 (interferon gamma receptor 1), thereby counteracting type-II interferon (IFN) signaling and establishing a feedback control mechanism to fine-tune macrophage-driven inflammation in MI.

Adverse remodeling post-MI presents a significant clinical challenge, necessitating early intervention. Excessive macrophage-driven inflammation leads to myocardial injury, suboptimal infarct repair, and maladaptive remodeling post-MI. The intrinsic mechanisms that curb macrophage immune responses, which are crucial for maintaining homeostasis and promoting effective infarct repair, remain poorly understood. Our study reveals that the E3 ubiquitin ligase RNF149 is highly expressed in cardiac macrophages within murine and human acute MI tissues. RNF149 deficiency exacerbates cardiac dysfunction and impairs infarct healing by increasing the infiltration of proinflammatory monocytes/macrophages and reducing reparative subsets. We report a mechanism wherein RNF149, transactivated by STAT1, mediates the ubiquitylation-dependent proteasomal degradation of IFNGR1, serving as a negative feedback regulator of type-II IFN signaling in macrophages and, thus, acting as a molecular brake on macrophage inflammation during MI. These findings highlight the therapeutic potential of targeting macrophage RNF149 to enhance cardiac function and improve the prognosis of patients with MI.

Nonstandard Abbreviations and Acronyms

AAV	adeno-associated virus
Ad	adenovirus
BM	bone marrow
BMDM	bone marrow–derived macrophage
CCR2	C-C motif chemokine receptor 2
HMGB1	high-mobility group box 1
IA	infarct area
IFN	interferon
IL	interleukin
JAK	Janus kinase
LUBAC	linear ubiquitin chain assembly complex
LV	left ventricular
MHC-II	major histocompatibility complex II
MI	myocardial infarction
Mo/MΦ	monocytes/macrophages
NIA	noninfarct area
RNF149	ring finger protein 149
RNF149KO	ring finger protein 149 knockout
TGF-β	transforming growth factor-β
TUNEL	TdT-mediated dUTP nick-end labeling
Tyr701	tyrosine residue 701
VEGF-α	vascular endothelial growth factor-α
WT	wild-type
α-SMA	α-smooth muscle actin

remodeling and heart failure, owing to compromised infarct repair, which is driven primarily by intense tissue inflammation and subsequently by its active suppression and resolution.[2,3] Consequently, interventions aimed at modulating the inflammatory and reparative responses hold the potential for averting post-MI heart failure.

Necrotic cells release danger-associated molecular patterns, which augment myeloid output to amplify the inflammatory response in MI tissue.[2,4] The direct sensing of danger-associated molecular patterns triggers transcriptional and epigenetic networks that facilitate the switch of myeloid cells from steady state to inflammatory programming.[3] Accumulating evidence, including ours, has demonstrated that infarct macrophages display distinct functional dynamics, playing a pivotal role in the postinfarction inflammatory and reparative

ORIGINAL RESEARCH

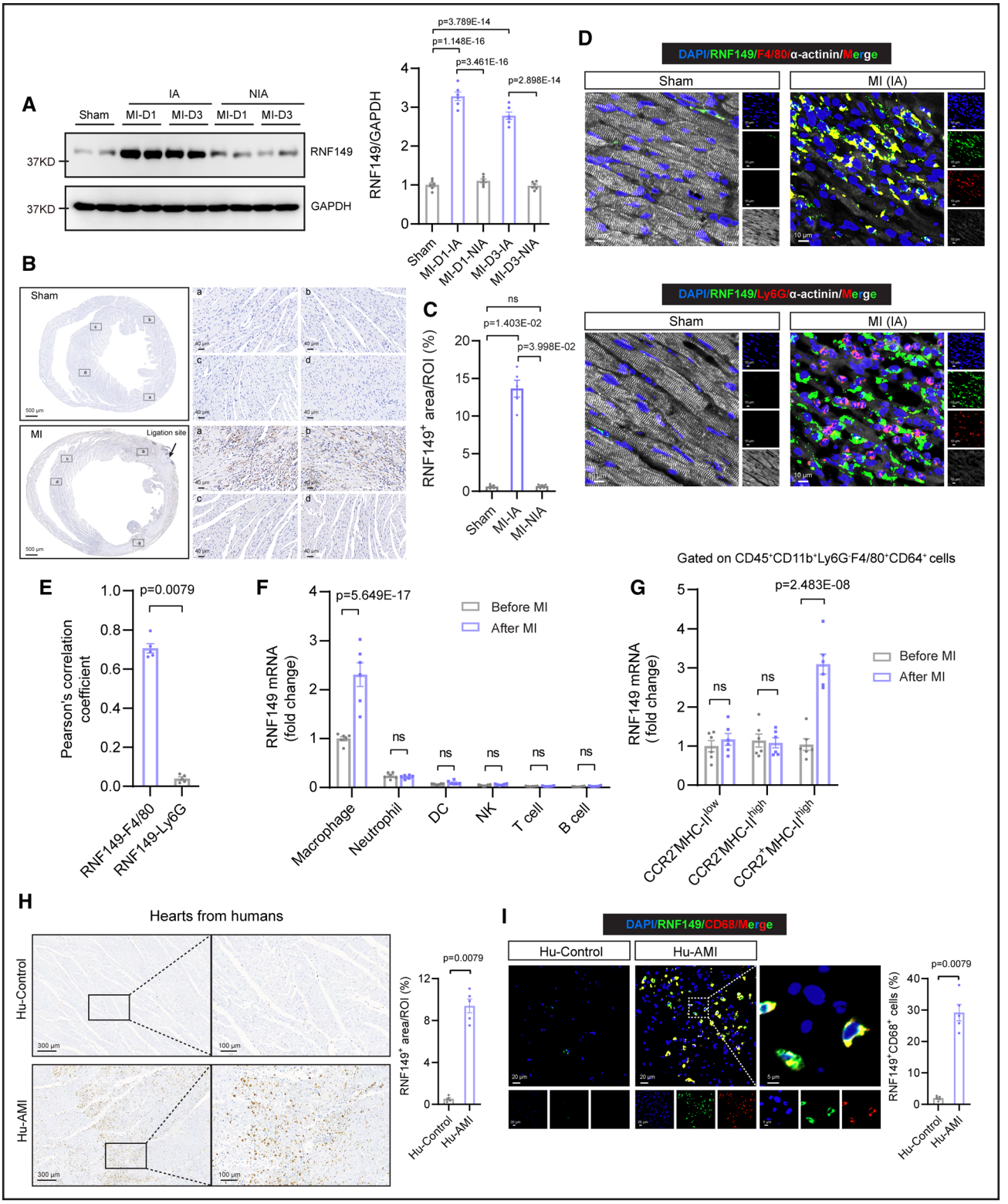

Figure 1. Macrophages highly expressing RNF149 (ring finger protein 149) infiltrate murine and human acute myocardial infarction (MI) tissue.

A, Immunoblot analysis of RNF149 expression in infarct and noninfarct areas of wild-type (WT)-MI hearts and sham controls (n=6). **B**, Overview and high-magnification images of immunohistochemical staining for RNF149 on cross sections of WT post-MI hearts and sham controls. **C**, Dot plot depicting quantified data of B (n=5). **D**, Immunofluorescence staining of RNF149, F4/80, Ly6G, and α-actinin in WT hearts before and 3 days after MI. **E**, Quantification of D (n=5). **F**, Analysis of RNF149 mRNA expression in leukocyte population isolated from WT hearts before and after MI (n=6). **G**, RNF149 mRNA levels in 3 cardiac macrophage subsets of WT hearts before and after MI (n=6). **H**, Immunohistochemistry for RNF149 in heart sections of patients with acute MI and control subjects without pathological or clinical evidence of heart (*Continued*)

processes.[2,3,5–8] In the early phase of MI, monocyte-derived macrophages exhibit proinflammatory signatures, secreting inflammatory cytokines and chemokines to generate inflammation.[4] In the later phase of MI, reparative macrophages accumulate in the infarct area (IA), exerting anti-inflammatory effects and contributing to tissue repair.[4] Uncontrolled inflammation exacerbates ischemic injury by destroying surviving border-area cardiomyocytes and hindering damaged tissue repair.[4] In contrast, tempering proinflammatory macrophage activation reduces cardiomyocyte necrosis and promotes wound healing post-MI.[4,6] An active coordinated program for resolution, orchestrated by the macrophages themselves, ensures tissue repair and homeostasis.[2,3] Therefore, the exploration of key molecules responsible for well-orchestrated macrophage–mediated inflammation may yield potential intervention targets for MI.[9]

Our prior investigations focused on delineating the signals that trigger the proinflammatory properties of macrophages under ischemic stress.[5–7] Exploring the intrinsic mechanisms that inhibit macrophage responsiveness to MI would enhance our understanding of the regulation of macrophage-associated inflammation. Ubiquitination, as a crucial protein posttranslational modification, widely participates in various stages of inflammatory response.[10,11] E3 ubiquitin ligases play a pivotal role in the ubiquitination process by specifically recognizing and binding to substrate proteins and transferring ubiquitin to these substrates.[12] Recent investigations have unveiled the capacity of certain E3 ligases to influence the degradation or functional activities of proteins implicated in innate immunity, thereby acting as safeguards against excessive immune responses.[10,11,13] However, in the context of MI, it remains unclear whether key E3 ligases exist to exert analogous regulatory effects on the proinflammatory activation of infarct macrophages.

In the present study, employing transcriptome analysis, we identified an E3 ligase termed RNF149 (ring finger protein 149) displaying high expression in murine and human infarct macrophages during the acute phase of MI. The role of RNF149 in cardiac ischemic injury was further explored utilizing RNF149 knockout (RNF149KO) mice. Our findings suggest that RNF149 controls the stability of substrate IFNGR1 (interferon gamma receptor 1) to promote the resolution of macrophage-driven inflammation, thereby preventing adverse remodeling after MI. In summary, our study reveals a posttranslational mechanism responsible for terminating the inflammatory response in the MI hearts.

METHODS

Data Availability

All data and detailed methods can be found in the Supplemental Material or provided upon reasonable request. Statistical analysis was performed following the Statistical Reporting Recommendations of *Circulation Research*. Please refer to the Expanded Methods and the Major Resources Table in the Supplemental Material.

RESULTS

Macrophages Highly Expressing RNF149 Infiltrate Murine and Human Acute MI Tissue

We first examine the expression alteration of E3 ligase genes in macrophages subjected to inflammatory stimuli using transcriptome data (Figure S1). Through integrated analysis of differentially expressed E3 ligase genes in cardiac macrophages pre- and post-MI, as well as in bone marrow–derived macrophages (BMDMs) before and after inflammatory insult, we identified 10 E3 ligase genes exhibiting significant upregulation in both infarct macrophages on the first day after MI and in BMDMs under proinflammatory activation (Figure S1). After scrutinizing the expression profiles of these 10 genes in the BioGPS database, RNF149 and TRIM13 emerged as potential candidate genes due to their high and specific expression in BMDMs and peritoneal macrophages, regardless of inflammatory stimulation, in comparison to other immune cells and cardiomyocytes (Figures S1 and S2). Subsequently, we validated RNF149 and TRIM13 expression in macrophages infiltrating the infarcted myocardium. Unlike RNF149, TRIM13 mRNA expression in cardiac macrophages exhibited similarity to that of T cells and did not demonstrate a 2-fold increase post-MI (Figure S3; Figure 1).

Immunoblot and immunohistochemistry demonstrated an elevated RNF149 expression in the IA but not in the noninfarct area of wild-type (WT) mouse hearts during the early phase of MI compared with sham controls (Figure 1A and 1C). This result aligns with the notion that immune cell infiltration primarily occurs in the infarct zone.[6] Additionally, immunofluorescence co-staining for RNF149 with F4/80 or Ly6G (lymphocyte antigen 6 family member G) in 3-day-old infarcts revealed the enrichment of RNF149 in macrophages but not in neutrophils (Figure 1D and 1E). By sorting immune cells from mouse hearts before and after MI, we identified a prevailing expression of RNF149 within macrophages compared with other leukocytic subtypes

Figure 1 Continued. disease (n=5). **I**, Immunofluorescence staining of RNF149 and CD68 (cluster of differentiation 68) in heart sections of patients with acute MI and control subjects (n=5). Data were analyzed using 1-way ANOVA with the Bonferroni multiple comparisons test (**A**), Kruskal-Wallis test with the Dunn post hoc test (**C**), 2-way ANOVA with the Bonferroni multiple comparisons test (**F** and **G**), and the Mann-Whitney *U* test (**E**, **H**, **I**). AMI indicates acute myocardial infarction; CD, cluster of differentiation; F4/80, adhesion G protein-coupled receptor E1; Hu, Human; IA, infarct area; Ly6G, lymphocyte antigen 6 family member G; NIA, noninfarct area; and ns, not significant.

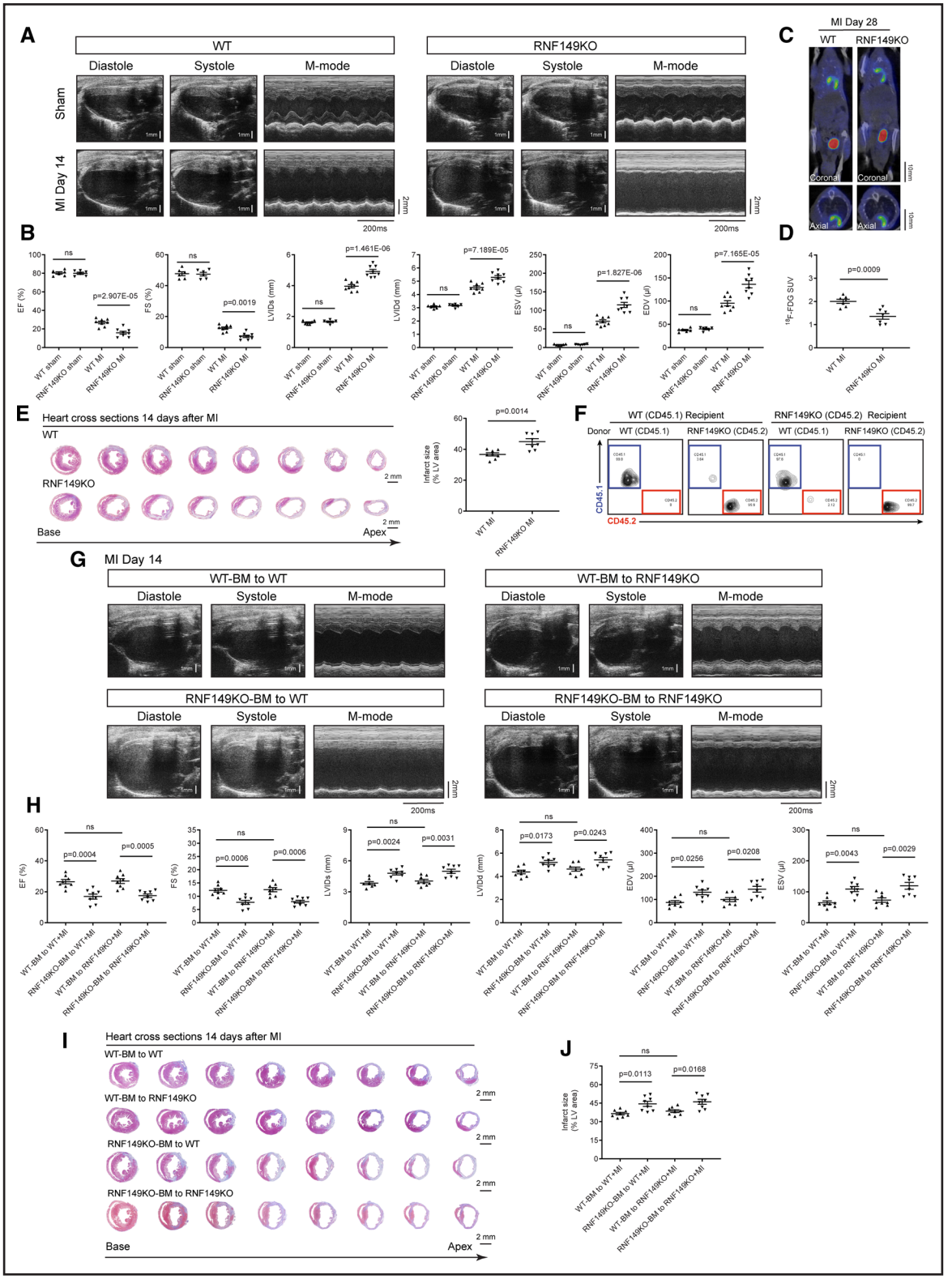

Figure 2. RNF149 (ring finger protein 149) knockout exacerbates myocardial dysfunction and adverse remodeling after myocardial infarction (MI).

A, Representative B-mode and M-mode echocardiograms from wild-type (WT) and RNF149 knockout (RNF149KO) mice following MI or sham surgery. **B**, Echocardiographic measurements of ejection fraction (EF), fractional shortening (FS), left ventricular internal diameter at end systole (LVIDs), left ventricular internal diameter at end diastole (LVIDd), end-systolic volume (ESV), and end-diastolic volume (EDV) in WT and RNF149KO hearts after sham operation (n=6) or 14 days after MI (n=8). **C**, Representative ^{18}F-fluorodeoxyglucose (^{18}F-FDG) positron emission tomography/computed tomography (PET/CT) images at 4 weeks after MI. **D**, Quantification of myocardial standardized uptake value (SUV) of ^{18}F-FDG in C (n=7). **E**, Masson trichrome staining for infarct measurements in RNF149KO and WT mice 14 days after MI (n=8). (*Continued*)

and observed an upregulation of RNF149 expression in infarct macrophages (Figure 1F; Figure S4). Furthermore, by classifying cardiac macrophages into 3 subsets based on their expression of MHC-II (major histocompatibility complex II) and CCR2 (C-C motif chemokine receptor 2), we observed a notable upregulation of RNF149 expression in MHC-II^{high}CCR2^{+} macrophages following MI, in comparison with MHC-II^{low}CCR2^{-} and MHC-II^{high}CCR2^{-} macrophage subpopulations (Figure 1G; Figure S5). Additionally, immunohistochemistry revealed an increase in RNF149 expression within human acute MI tissue (Figure 1H). Our analysis also unveiled the infiltration of RNF149^{+}CD68^{+} macrophages in the acutely infarcted human myocardium (Figure 1I). Finally, we confirmed the release of the well-established danger-associated molecular pattern, HMGB1 (high-mobility group box 1),[4] from the nuclei in the infarcted hearts (Figure S6). In summary, these findings elucidate the accumulation of macrophages highly expressing RNF149 within the infarcted myocardium during the early inflammatory phase of MI, suggesting the involvement of RNF149 in the regulation of macrophage-driven inflammation in MI.

RNF149 Knockout Exacerbates Myocardial Dysfunction and Adverse Remodeling After MI

The function of RNF149 in MI remains unclear. Thus, we generated RNF149KO mice and confirmed the depletion of RNF149 in the MI hearts of these mice (Figure S7). Echocardiography indicated that RNF149 loss did not alter baseline heart rate, cardiac geometry, or myocardial function (Table S1). To determine the functional role of RNF149 in MI, RNF149KO and WT control male mice were subjected to MI at 9 weeks of age. Echocardiographic parameters, including left ventricular (LV) fractional shortening and ejection fraction, exhibited a marked reduction in RNF149KO mice compared with WT controls 14 days after MI (Figure 2A and 2B; Table S2). Besides, the expansion of LV chamber dilation was notably exacerbated in RNF149KO mice 2 weeks after MI, as evidenced by an increase in end-diastolic volume and LV internal diameter at end diastole (Figure 2A and 2B; Table S2). Meanwhile, representative ^{18}F-fluorodeoxyglucose positron emission tomography/computed tomography scanning suggested significantly reduced myocardial viability in RNF149KO mice after MI (Figure 2C and 2D). Furthermore, Masson trichrome staining of serial heart cross sections revealed an augmentation in the infarct size of RNF149KO mice at 14 days after MI (Figure 2E). Collectively, our data illustrate the detrimental effects of RNF149 loss on MI.

RNF149 Expressed on Bone Marrow–Derived Cells Contributes to MI

To further explore the significance of RNF149 expression in myeloid cells infiltrating the MI tissue, we conducted bone marrow transplantation experiments involving both RNF149KO and WT mice. Given that RNF149KO mice had a C57BL/6 background expressing the CD45.2 allele, we used a C57BL/6 substrain expressing the CD45.1 allele (C57BL/6-CD45.1), identical to the WT mice, to assess bone marrow (BM) reconstitution (Figure 2F). Flow cytometric analysis confirmed that CD45.1-WT mice expressed the CD45.1 allele, whereas RNF149KO mice expressed CD45.2 (Figure 2F). Eight weeks following the bone marrow transplantations, the successful reconstitution of recipient mice's BM with donor BM cells was ascertained by examining peripheral blood cells through flow cytometry (Figure 2F). Subsequently, recipient mice that underwent successful bone marrow transplantation procedures were subjected to MI. We observed a worsened cardiac dysfunction, manifested by a reduction in fractional shortening and ejection fraction, along with an increase in LV internal diameter at end-diastole and end-diastolic volumes, in the RNF149KO-BM-to-WT group compared with the WT-BM-to-WT mice after MI (Figure 2G and 2H; Table S3). In contrast, cardiac function exhibited significant improvement in RNF149KO mice transplanted with WT BM (Figure 2G and 2H; Table S3). Additionally, the transplantation of RNF149KO BM–derived cells to WT mice resulted in an increase in infarct size compared with WT mice transplanted with WT BM. Conversely, the transplantation of WT BM-derived cells to RNF149KO mice led to a considerable decrease in infarct size compared with RNF149KO mice transplanted with RNF149KO BM–derived cells (Figure 2I and 2J). These findings highlight the critical contribution of RNF149 from BM-derived cells to cardiac injury and remodeling post-MI.

We further established a BM macrophage–specific RNF149-knockdown murine model. An adeno-associated virus (AAV)–encoding RNF149-short hairpin RNA under the control of the macrophage-specific F4/80

Figure 2 Continued. **F**, Flow cytometric analysis of CD45.1^{+} and CD45.2^{+} cells in the peripheral blood of CD45.1 (WT) and CD45.2 (RNF149KO) mice transplanted with bone marrow (BM) cells from CD45.1 (WT) or CD45.2 (RNF149KO) mice (n=3). **G**, Representative B-mode and M-mode echocardiograms from mice with BM transplantation described in **F**, 14 days after MI. **H**, Summarized data of echocardiographic measurements in **G** (n=8). **I**, Representative Masson trichrome staining of heart cross sections from mice with BM transplantation described in **F** 14 days after MI. **J**, Summarized data of infarct size measured from **I** (n=8). Data were analyzed using 2-way ANOVA with the Bonferroni multiple comparisons test (**B**, **H**, and **J**) and the unpaired 2-tailed Student *t* test (**C** and **E**). CD indicates cluster of differentiation; LV, left ventricular; ns, not significant; and PET/CT, positron emission tomography/computed tomography.

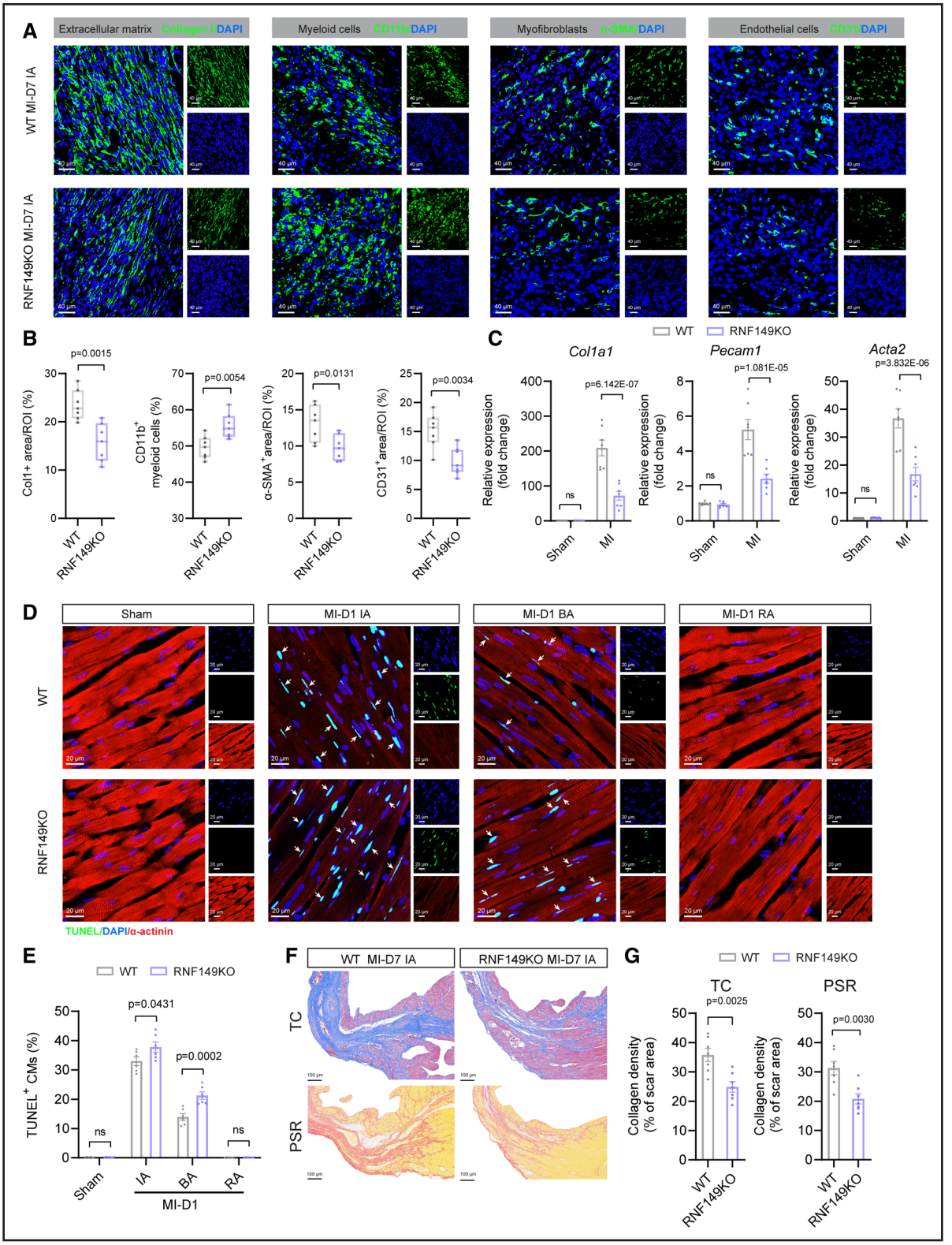

Figure 3. RNF149 (ring finger protein 149) deficiency impairs postinfarction cardiac repair and aggravates myocardial apoptosis in myocardial infarction (MI) tissue.

A, Immunofluorescence staining of collagen I, CD11b, α-SMA (α-smooth muscle actin), and CD31 in wild-type (WT) and RNF149 knockout (RNF149KO) infarcts at 7 days after MI. **B**, Dot plots showing the quantified data of **A** (n=7), with each dot representing the mean of data from 10 to 15 images in 1 mouse. **C**, mRNA levels of *Col1a1*, *Pecam1*, and *Acta2* in WT and RNF149KO hearts after sham operation or 7 days after MI (n=7). **D**, In situ TdT-mediated dUTP nick-end labeling (TUNEL)/α-actinin double staining on RNF149KO and WT hearts after sham operation or 1 day after MI to detect myocardial apoptosis. TUNEL-positive cardiomyocytes (CMs) are indicated by arrows. **E**, Dot plots (*Continued*)

promoter was administered via intra-BM injection to target RNF149-short hairpin RNA expression specifically to BM macrophages in mice (Figure S8), as previously described.[14–16] Confirmation of RNF149 knockdown in macrophages of AAV-infected mice was achieved through qPCR (quantitative polymerase chain reaction) (Figure S8). Echocardiography showed that RNF149 knockdown in macrophages exacerbated cardiac dysfunction in mouse models of MI (Figure S8; Table S4). Collectively, these results demonstrate the deleterious effect of macrophage RNF149 loss on MI.

RNF149 Loss Aggravates Myocardial IR Injury

In clinical practice, prompt reperfusion therapy has been shown to improve the clinical outcomes of patients with acute MI. Thus, we further investigated the functional implications of RNF149 in myocardial ischemia/reperfusion (IR) injury. With similar size of area at risk, the IA relative to the area at risk exhibited a notably higher ratio in RNF149KO mice compared with the WT counterparts, 48 hours after reperfusion (Figure S9). Consistent with these findings, 2,3,5-triphenyltetrazolium chloride staining revealed larger sized infarcts in RNF149KO mice after IR (Figure S9). In tandem, the absence of RNF149 resulted in an increase in end-systolic volume and left ventricular internal diameter at end systoles, coupled with a decrease in ejection fraction and fractional shortening, in comparison with the WT mice, 4 days following IR (Figure S9). These findings collectively demonstrate the pivotal role of RNF149 in myocardial IR injury.

RNF149 Overexpression in Cardiac Macrophages Improves Cardiac Function in a Mouse Model of MI

The use of adenovirus (Ad) vectors for delivering therapeutic genes to the hearts has attracted considerable attention. To explore the potential benefits of RNF149 during MI, we used an adenoviral vector encoding RNF149 under the control of macrophage CD68 (cluster of differentiation 68) promoter (AdRNF149) via intramyocardial injection at a singular dose post-MI to induce transient overexpression of RNF149 specifically in cardiac macrophages, as previously described.[17,18] RNF149 expression in infarct macrophages demonstrated a marked elevation in AdRNF149-treated mice compared with those treated with Adnull (Figure S10). Our results indicated that the overexpression of RNF149 in macrophages significantly mitigated MI-induced cardiac dysfunction, suggesting a promising therapeutic role for RNF149 in MI (Figure S10; Table S5).

Absence of RNF149 Impairs Postinfarction Cardiac Repair and Aggravates Myocardial Injury in MI Tissue

The early inflammatory phase post-MI is characterized by myocardial ischemic injury and leukocyte infiltration, followed by inflammation resolution and infarct healing. We set out to investigate the impact of RNF149 deficiency on postinfarction cardiac repair. We observed a greater accumulation of $CD11b^+$ myeloid cells in the infarct zone of RNF149KO hearts compared with WT controls, 7 days after MI (Figure 3A and 3B). Additionally, 7-day-old infarcts of RNF149KO mice exhibited reduced collagen I deposition (Figure 3A and 3B). Notably, we detected fewer α-SMA^+ (α-smooth muscle actin) myofibroblasts in the IA of RNF149KO hearts compared with WT controls, 1 week after MI (Figure 3A and 3B). Furthermore, 7-day-old infarcts of RNF149KO mice exhibited reduced angiogenesis, as reflected by a significant decrease in the number of $CD31^+$ endothelial cells (Figure 3A and 3B). In parallel, a decrease in mRNA levels of *Col1a1*, *Pecam1*, and *Acta2* was observed in the IA of RNF149KO hearts 1 week after MI, in comparison with the WT controls (Figure 3C). However, it is worth noting that RNF149 deficiency had a minimal impact on myeloid cell infiltration, collagen I deposition, angiogenesis, and myofibroblast differentiation in the noninfarct zone (Figure S11). Prior studies have emphasized the significance of hyperactive inflammatory responses and apoptosis as key mechanisms contributing to early stage ischemic cardiac injury in MI.[6,19] Consequently, we conducted a TdT-mediated dUTP nick-end labeling (TUNEL) assay to detect myocardial apoptosis on the first day following MI. In comparison with WT controls, we observed a significant increase in apoptotic cardiomyocytes ($TUNEL^+\alpha$-$actinin^+$) in the border area of RNF149KO hearts on the 1 day after MI (Figure 3D and 3E). This finding aligns with our earlier observation of increased infarct size in RNF149KO mice (Figure 2E). We also quantified collagen deposition using Masson trichrome staining and Picrosirius red staining. We found that the collagen density in the IA was significantly lower in RNF149KO hearts compared with WT hearts 7 days after MI (Figure 3F and 3G). The formation of collagen-scarce scars in RNF149KO infarcted hearts indicates impaired postinfarction repair. However, the

Figure 3 Continued. showing the quantified data of D (n=6). **F**, Masson trichrome (TC) and Picrosirius red (PSR) staining of heart transverse sections to detect collagen within the scar of WT and RNF149KO hearts 7 days after MI. **G**, Collagen density in **F** measured as the total collagen area divided by scar area examined (n=7). Data were analyzed using the unpaired 2-tailed Student *t* test (**B** and **G**) and 2-way ANOVA with the Bonferroni multiple comparisons test (**C** and **E**). BA indicates border area; CD, cluster of differentiation; DAPI, 4′,6-diamidino-2-phenylindole IA, infarct area; ns, not significant; and RA, remote area.

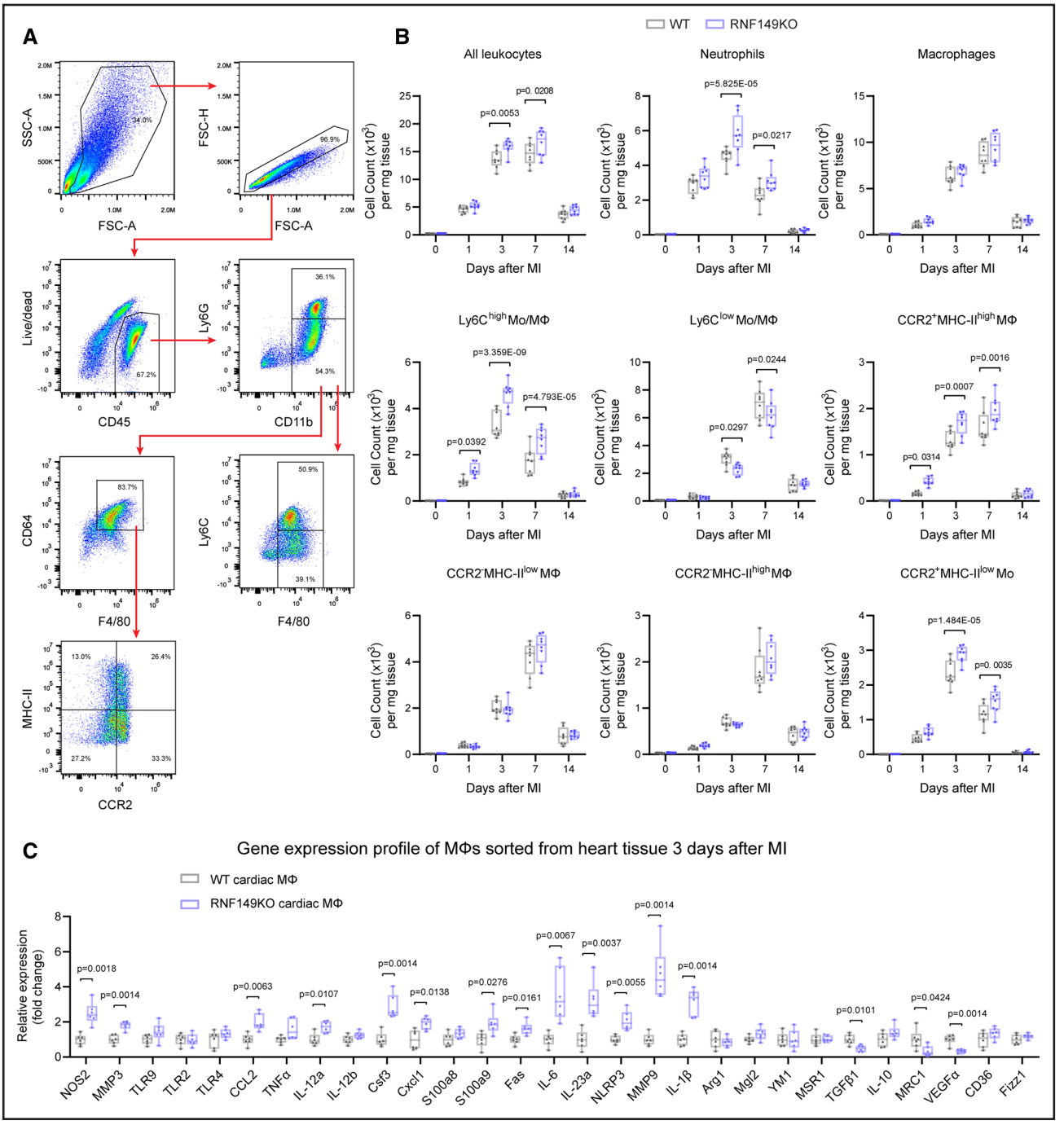

Figure 4. RNF149 (ring finger protein 149) loss-of-function enhances inflammatory macrophage infiltration in myocardial infarction (MI) hearts.

A, Flow cytometry gating strategy for cardiac leukocyte population 3 days after MI. **B**, Flow cytometry-based quantification of cell numbers of total leukocytes, neutrophils, macrophages, Ly6C^{high} monocytes/macrophages (Mo/MΦ), Ly-6C^{low} Mo/MΦ, CCR2^{+}MHC-II^{high} MΦ, CCR2^{-}MHC-II^{high} MΦ, CCR2^{-}MHC-II^{low} MΦ, and CCR2^{+}MHC-II^{low} Mo in wild-type (WT) and RNF149 knockout (RNF149KO) hearts before and 1, 3, 7, and 14 days after MI; n=8. **C**, mRNA levels of major proinflammatory and anti-inflammatory genes in macrophages (CD45^{+}CD11b^{+}Ly6G^{-}F4/80^{+}CD64^{+}) sorted from WT and RNF149KO infarcts on day 3 after MI; n=5. Data in **B** were analyzed using 2-way ANOVA with the Bonferroni multiple comparisons test. Data in **C** were analyzed by the multiple unpaired *t* tests with the Benjamini and Hochberg false discovery rate (FDR) correction. CCR2 indicates C-C motif chemokine receptor 2; CD, cluster of differentiation; FSC, forward scatter; Ly6C, lymphocyte antigen 6 family member C; MHC-II, major histocompatibility complex II; and SSC-A, side scatter area.

collagen content in the noninfarct zone was comparable between WT and RNF149KO mice (Figure S12). In summary, these findings collectively underscore that the absence of RNF149 exacerbates ischemic myocardial injury, retards the resolution of inflammation, and impairs postinfarction cardiac repair.

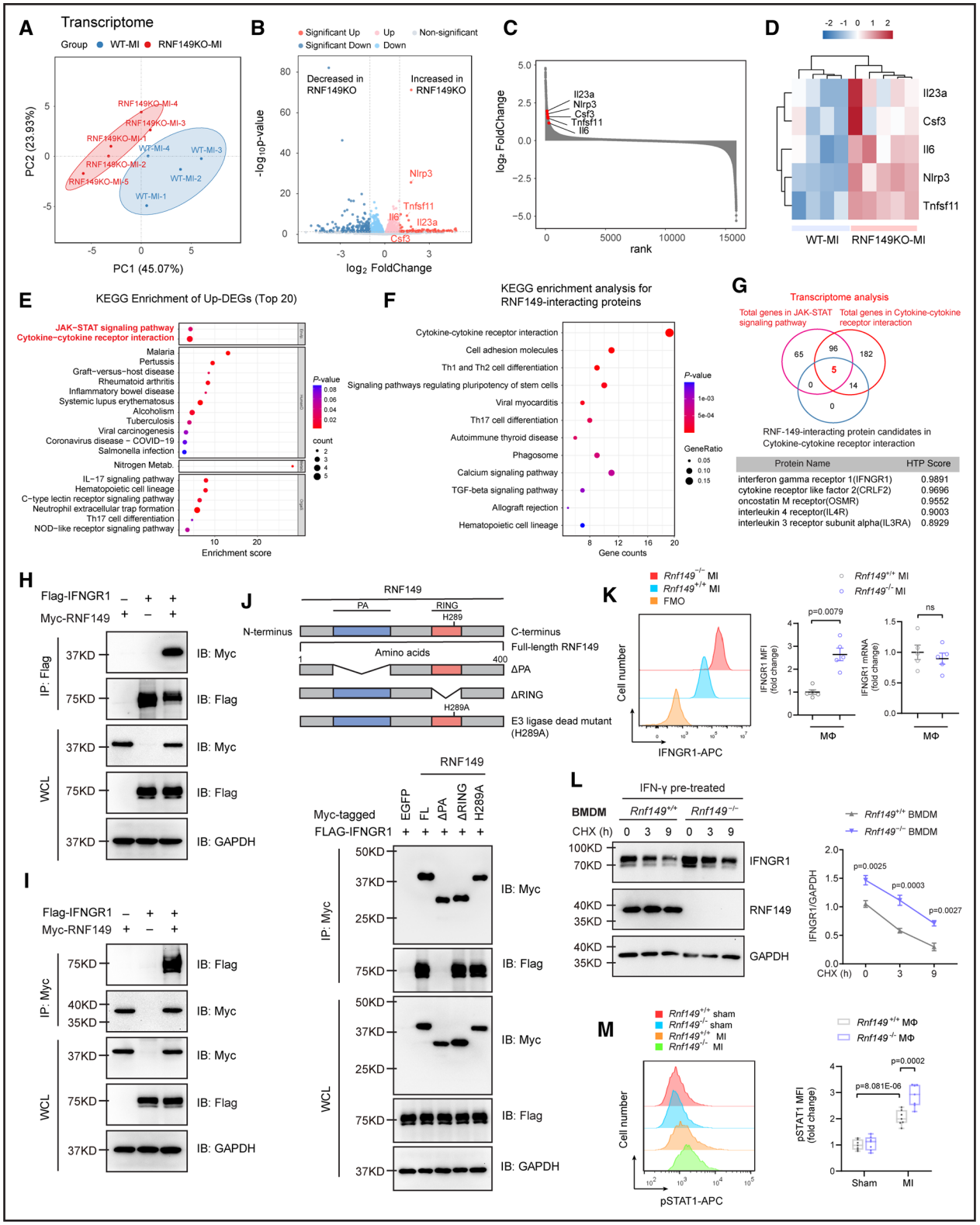

Figure 5. RNF149 (ring finger protein 149) interacts with IFNGR1 (interferon gamma receptor 1) to control macrophage-driven inflammation in myocardial infarction (MI).

A, Principal component analysis of transcriptome expression values from wild-type (WT) and RNF149 knockout (RNF149KO) hearts at 3 days after MI; n=4 for WT and 5 for RNF149KO. **B**, Volcano plot displaying the differentially expressed genes (DEGs, absolute fold change ≥2 and $P<0.05$) between RNF149KO MI hearts and WT controls. The horizontal dash line represents a P value of 0.05, and the vertical dash lines correspond to 2-fold upregulation and downregulation. **C**, Genes ranked by the $\log_2$-fold change between RNF149KO MI hearts and WT controls. **D**, Heatmap of upregulated DEGs relevant to inflammation in RNF149KO MI hearts. **E**, Kyoto Encyclopedia of Genes and Genomes (KEGG) enrichment analysis of upregulated DEGs in RNF149KO MI hearts. The top 20 enriched pathways are listed. **F**, KEGG enrichment (*Continued*)

RNF149 Loss-of-Function Enhances Inflammatory Macrophage Infiltration After MI

To gain a deeper understanding of the mechanisms underlying the worsened outcomes in RNF149KO mice post-MI, we examined the impact of RNF149 loss on the infiltration of cardiac neutrophils and monocytes/macrophages (Mo/MΦ) using flow cytometric gating strategies as previously reported.[6] Ly6C (lymphocyte antigen 6 family member C)^{high} Mo/MΦ and MHC-II^{high}CCR2^{+} macrophages are known to exhibit proinflammatory properties, accumulate early in the infarcted myocardium, and contribute to inflammation. Conversely, Ly6C^{low} Mo/MΦ primarily represents reparative subsets and participates in the later stage of cardiac repair. At baseline, the profiles of myeloid cells in WT and RNF149KO hearts exhibited a notable similarity (Figure 4A and 4B). However, the absence of RNF149 led to a moderate increase in the infiltration of MHC-II^{high}CCR2^{+} macrophages and Ly6C^{high} Mo/MΦ at 1 day after MI. RNF149KO infarcts displayed a notably increased infiltration of Ly6C^{high} Mo/MΦ and neutrophils, alongside the reduced presence of reparative Ly6C^{low} Mo/MΦ, in comparison to WT controls, at day 3 after MI. Moreover, RNF149$^{-/-}$ hearts exhibited elevated levels of MHC-II^{low}CCR2^{+} monocytes and MHC-II^{high}CCR2^{+} macrophages post-MI (Figure 4A and 4B), indicating prolonged inflammation due to RNF149 deficiency.

We further analyzed the expression profiles of major inflammation-associated genes in infarct macrophages. Our findings revealed that macrophages from RNF149KO infarcts exhibited a heightened inflammatory transcriptional signature, as evidenced by upregulation of proinflammatory genes, including *Csf3* (colony stimulating factor 3), *IL* (interleukin)*-23a*, *IL-6*, *IL-1β*, *Ccl2*, *Cxcl1*, *NOS2* (type 2 nitric oxide synthase), and *MMP9* (matrix metallopeptidase 9), among others (Figure 4C). Moreover, infarct macrophages lacking RNF149 expressed decreased levels of anti-inflammatory genes, such as *TGF-β* (transforming growth factor-β) and vascular *VEGF-α* (vascular endothelial growth factor-α; Figure 4C). Collectively, these findings indicate that RNF149 deletion resulted in prolonged inflammation and impeded post-MI inflammation resolution.

RNF149 Interacts With IFNGR1 to Control Macrophage-Driven Inflammation in MI

Subsequently, we conducted transcriptome to comprehensively analyze genome-wide gene expression profiles in RNF149KO and WT infarcted hearts at 3 days after MI (Figure 5A). Among the differentially expressed genes, we observed significant upregulation of essential inflammatory genes, including *Csf3*, *IL-23a*, *IL-6*, *Nlrp3*, and *Tnfsf11* (Figure 5B and 5D), within the top 20 enriched pathways associated with inflammation in RNF149KO infarcted hearts (ie, JAK [Janus kinase]-STAT (signal transducer and activator of transcription) signaling pathway, cytokine-cytokine receptor interaction, C-type lectin receptor signaling pathway, and NOD (nucleotide-binding and oligomerization domain)-like receptor signaling pathway; Figure 5E). We recognize the variability in the expression of the elevated *IL-23a* and *Csf3* genes in the RNF149KO mice and acknowledge the potential impact of outliers on the interpretation of the result. The alterations in mRNA expression of *Csf3*, *IL-23a*, *IL-6*, *Nlrp3*, and *Tnfsf11* in RNF149KO infarcts were further confirmed by the qPCR analysis (Figure S13).

Given that RNF149 is a substrate-recognizing E3 ligase, we analyzed the protein interactome of RNF149 through co-immunoprecipitation/mass spectrometry from the BioGRID database (Table S6). With potential RNF149 interacting proteins, we perform Kyoto Encyclopedia of Genes and Genomes enrichment analysis (Figure 5F; Table S7).[20] To decipher the key interacting protein by which RNF149 modulates downstream signaling pathways identified via transcriptome, we conducted Venn diagram analysis to delineate the intersecting set of RNF149-binding protein candidates in the top 1 enriched pathway identified through co-immunoprecipitation/mass spectrometry and the total genes within the top-ranking enriched pathways identified through transcriptome, namely, the JAK-STAT signaling pathway and

Figure 5 Continued. analysis based on RNF149-interacting proteins identified from co-immunoprecipitation/mass spectrometry (co-IP/MS) in the BioGRID database. **G**, Venn diagram delineating the intersection of RNF149-binding protein candidates in the top 1 enriched pathway identified in **F** and the total genes within the top-ranking enriched pathways identified in **E**, that is, JAK (Janus kinase)-STAT (signal transducer and activator of transcription) signaling pathway and cytokine-cytokine receptor interaction. **H** and **I**, Immunoprecipitation in HEK293T cells transfected with Flag-IFNGR1 and Myc-RNF149 using anti-Flag (**H**) or anti-Myc (**I**) antibody, followed by immunoblot analysis with indicated antibodies. **J**, Immunoprecipitation in HEK293T cells cotransfected with Flag-IFNGR1 and truncated Myc-RNF149 or catalytically inactive RNF149 (H289A) using an anti-Myc antibody, followed by immunoblot analysis with indicated antibodies. **K**, IFNGR1 expression in macrophages from WT and RNF149KO MI hearts measured by flow cytometry and qPCR (quantitative polymerase chain reaction). **L**, Immunoblot analysis of IFNGR1 in *Rnf149*$^{+/+}$ and *Rnf149*$^{-/-}$ bone marrow–derived macrophages (BMDMs) treated with cycloheximide (CHX) for the indicated durations after stimulation with IFN (interferon)-γ for 4 hours. **M**, pY701-STAT1 expression in *Rnf149*$^{+/+}$ and *Rnf149*$^{-/-}$ cardiac macrophages 3 days after MI (n=7). *P* value in **B** was calculated using DESeq2 in R (v 3.2.0) based on the negative binomial distribution test. *P* values in **E** and **F** were calculated using R based on the hypergeometric distribution test. Data were analyzed using the Mann-Whitney *U* test (**K**), repeated measures 2-way ANOVA with the Bonferroni multiple comparisons test (**L**), and 2-way ANOVA with the Bonferroni multiple comparisons test (**M**). CD indicates cluster of differentiation; Csf3, colony stimulating factor 3; FMO, fluorescence minus one; HTP, high throughput; IL, interleukin; MFI, mean fluorescence intensity; Myc, myelocytomatosis oncogene; Nlrp3, NOD-, leucine-rich repeats- and pyrin domain-containing protein 3; PA, protease-associated; pY701, phosphorylation at tyrosine 701; qPCR, quantitative polymerase chain reaction; STAT, signal transducer and activator of transcription; TGF, transforming growth factor; and Tnfsf11, tumor necrosis factor superfamily member 11.

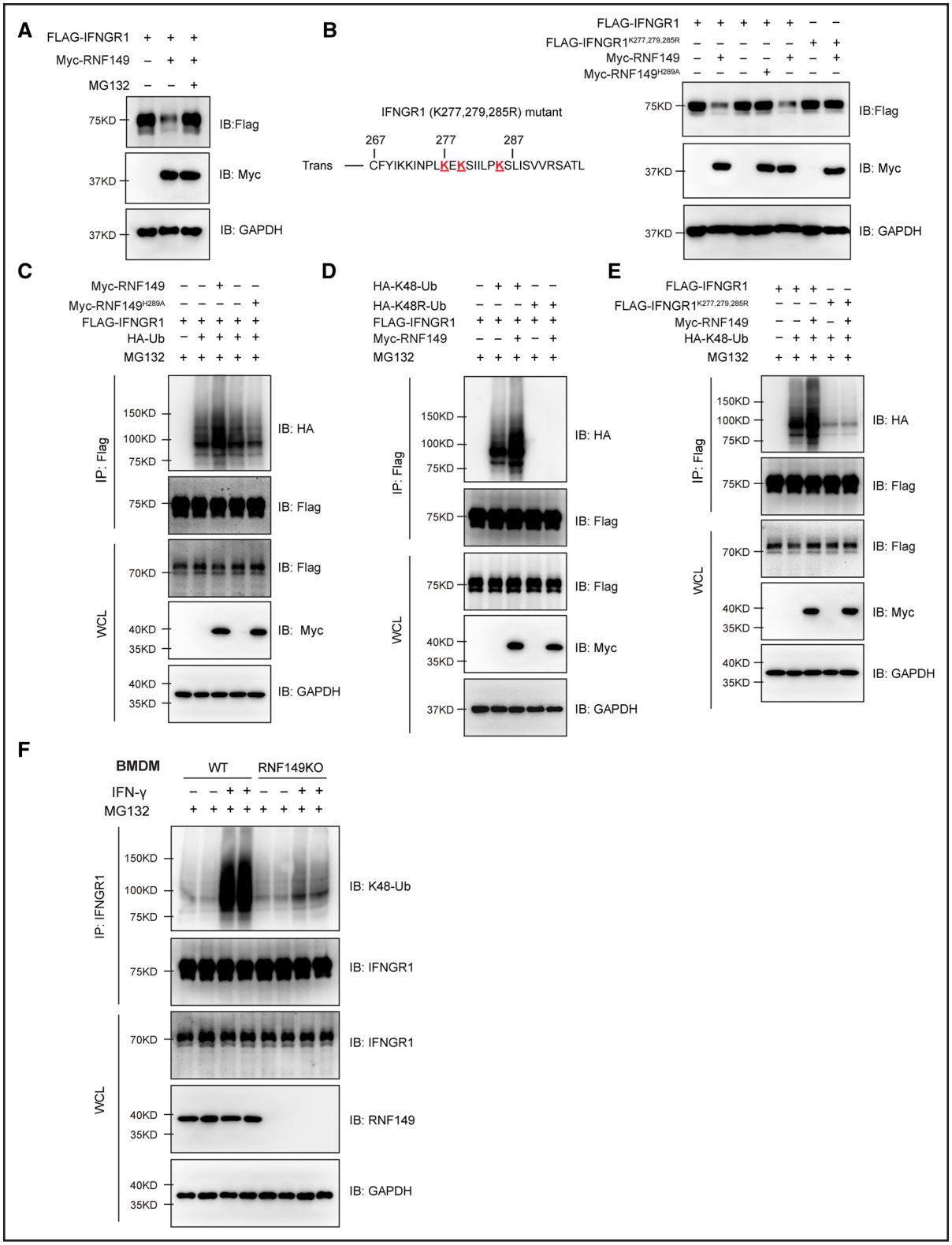

Figure 6. RNF149 (ring finger protein 149) drives proteasomal degradation of IFNGR1 (interferon gamma receptor 1) through K48-linked polyubiquitination.

A, Immunoblot analysis of IFNGR1 expression in HEK293T cells transfected with RNF149 and treated or not with MG132. **B**, Primary sequence of the IFNGR1 cytoplasmic juxtamembrane (JM) region (**left**). Lysine residues underlined are putative ubiquitin acceptor sites. Immunoblot analysis of HEK293T cells cotransfected with Myc-tagged RNF149 or RNF149^{H289A} mutant, along with Flag-tagged IFNGR1 or IFNGR1^{K277,279,285R} mutant to determine RNF149 as an E3 ligase for IFNGR1 and the role of putative ubiquitin acceptor sites on IFNGR1 degradation (**right**). **C**, Co-immunoprecipitation (co-IP) analysis of IFNGR1 ubiquitination in HEK293T cells cotransfected with Flag-IFNGR1 and HA-Ub, along with Myc-tagged RNF149 or RNF149^{H289A} mutant. **D**, The co-IP analysis of IFNGR1 ubiquitination (*Continued*)

cytokine-cytokine receptor interaction. Notably, IFNGR1 emerged as the top-ranked interacting protein candidate within the intersecting set (Figure 5G). Moreover, transcriptome analysis revealed that the mRNA levels of the 5 interacting protein candidates within the intersecting set remained minimally altered in RNF149KO infarcted hearts (Table S8). Therefore, we sought to validate IFNGR1 as a bona fide substrate of RNF149. We first conducted reciprocal co-immunoprecipitation experiments. Notably, RNF149 indeed interacted with IFNGR1 (Figure 5H). The interaction between RNF149 and IFNGR1 was further confirmed by a reverse IP experiment (Figure 5I). To further delineate the domain of RNF149 that interacts with IFNGR1, truncated RNF149 and RNF149 with catalytic site mutation (H289A) underwent co-immunoprecipitation analysis with IFNGR1. The protease-associated (PA) domain (67-175 amino acids [aa]) of RNF149 was identified as essential for its interaction with IFNGR1 (Figure 5J). Neither the RING domain nor the catalytic site was necessary for RNF149's binding with IFNGR1 (Figure 5J).

IFNGR1 serves as a crucial receptor protein in the type-II IFN (interferon) signaling pathway. Upon stimulation by IFN-γ, IFNGR1 activates the JAK1 kinase, culminating in STAT1 phosphorylation and subsequent induction of numerous inflammatory genes.[21] Initially, we examined the temporal dynamics of IFNGR1 and pSTAT1 (phosphorylated signal transducer and activator of transcription 1) expression in cardiac macrophage and myocardial IFN-γ levels after MI. We observed an early and gradual increase of IFN-γ levels in the infarcted hearts. Conversely, the induction of IFNGR1 and pY701 (phosphorylation at tyrosine 701)-STAT1 expression in infarct macrophages peaked on 1 day after MI and diminished by day 7 (Figure S14). These findings indicate the early activation of the IFNGR1/STAT1 signaling pathway in infarct macrophages, contributing to their proinflammatory activation.

To determine whether RNF149 functions as an E3 ligase to promote IFNGR1 degradation, we assessed the expression of IFNGR1 in infarct macrophages derived from WT and RNF149KO hearts. We observed a strong induction of IFNGR1 expression in RNF149KO macrophages, underscoring the pivotal role of RNF149 in restraining IFNGR1 expression (Figure 5K). However, RNF149 loss did not affect the IFNGR1 mRNA level (Figure 5K). In addition, RNF149 deficiency significantly decreased the degradation rate of endogenous IFNGR1 protein in BMDMs in the presence of the translation inhibitor cycloheximide (Figure 5L). These results suggest that RNF149 regulates IFNGR1 at the posttranslational level. Consistent with these observations, RNF149KO augmented the early induction of pY701-STAT1 in infarct macrophages (Figure 5M).

RNF149 Drives Proteasomal Degradation of IFNGR1 Through K48-Linked Polyubiquitination

As expected, exogenously expressed IFNGR1 was degraded by overexpressed RNF149 in HEK293 cells, which was also abrogated by the application of the proteasome inhibitor MG132, indicating that RNF149 mediates proteasomal degradation of IFNGR1 (Figure 6A). The histidine residue (amino acid 289) within the RING domain of E3 ligases is highly conserved and is essential for accepting ubiquitin from E2.[22] To further validate the function of RNF149 as an E3 ligase responsible for IFNGR1 degradation, we constructed a plasmid carrying a RING mutant form of RNF149 (RNF149^{H289A}), which lacks E3 ligase activity. We found that the RNF149 catalytic site mutant (RNF149^{H289A}) failed to induce the degradation of the IFNGR1 protein (Figure 6B). Considering that membrane-proximal lysine (K) residues 277, 279, and 285 of IFNGR1 are the most frequent targets of ubiquitination,[23,24] we made lysine-to-arginine point mutations to confirm the role of RNF149-mediated ubiquitination in IFNGR1 stability. Notably, RNF149 did not elicit reduced expression of IFNGR1^{K277,279,285R} (Figure 6B).

Our investigation delved into the authenticity of IFNGR1 as a substrate of RNF149. We conducted transfections of IFNGR1, RNF149, and ubiquitin into HEK293T cells. Our findings indicate that overexpression of RNF149 increased the polyubiquitination level of IFNGR1 (Figure 6C). Furthermore, the RNF149 catalytic site mutant (RNF149^{H289A}) construct failed to promote IFNGR1 polyubiquitination (Figure 6C). K48-linked polyubiquitination primarily mediates the proteasomal degradation of substrate proteins.[10] Thus, we transfected HEK293T cells with RNF149, IFNGR1, K48-specific ubiquitin (all lysine residues, except for K48, were mutated to arginine), or K48 mutant (K48R) ubiquitin. RNF149 promoted the polyubiquitination of IFNGR1 in the presence of K48-specific ubiquitin. However, RNF149 did not catalyze IFNGR1 polyubiquitination in the presence of K48R mutant ubiquitin, which harbored a lysine-to-arginine substitution at position 48 (Figure 6D). Besides, the IFNGR1^{K277,279,285R} exhibited a reduced level of K48-linked polyubiquitination when compared with the WT IFNGR1 (Figure 6E). We further analyzed the endogenous ubiquitination of IFNGR1 in *Rnf149*$^{+/+}$ and *Rnf149*$^{-/-}$ BMDMs in response to IFN-γ. Strikingly, K48-linked

Figure 6 Continued. in HEK293T cells cotransfected with Flag-IFNGR1 and Myc-RNF149, along with HA-K48-Ub or the mutant ubiquitin HA-K48R-Ub. **E**, The co-IP analysis of IFNGR1 ubiquitination in HEK293T cells cotransfected with Myc-RNF149 and HA-K48-Ub, along with Flag-tagged IFNGR1 or IFNGR1^{K277,279,285R} mutant. **F**, The co-IP analysis of K48-linked ubiquitination of endogenous IFNGR1 in *Rnf149*$^{+/+}$ or *Rnf149*$^{-/-}$ bone marrow–derived macrophages (BMDMs) stimulated or not with IFN (interferon)-γ at the presence of MG132. Data are representative of at least 3 independent experiments. HA-Ub indicates hemagglutinin-ubiquitin; Myc, myelocytomatosis oncogene; Trans, transmembrane domain; and WCL, whole cell lysate.

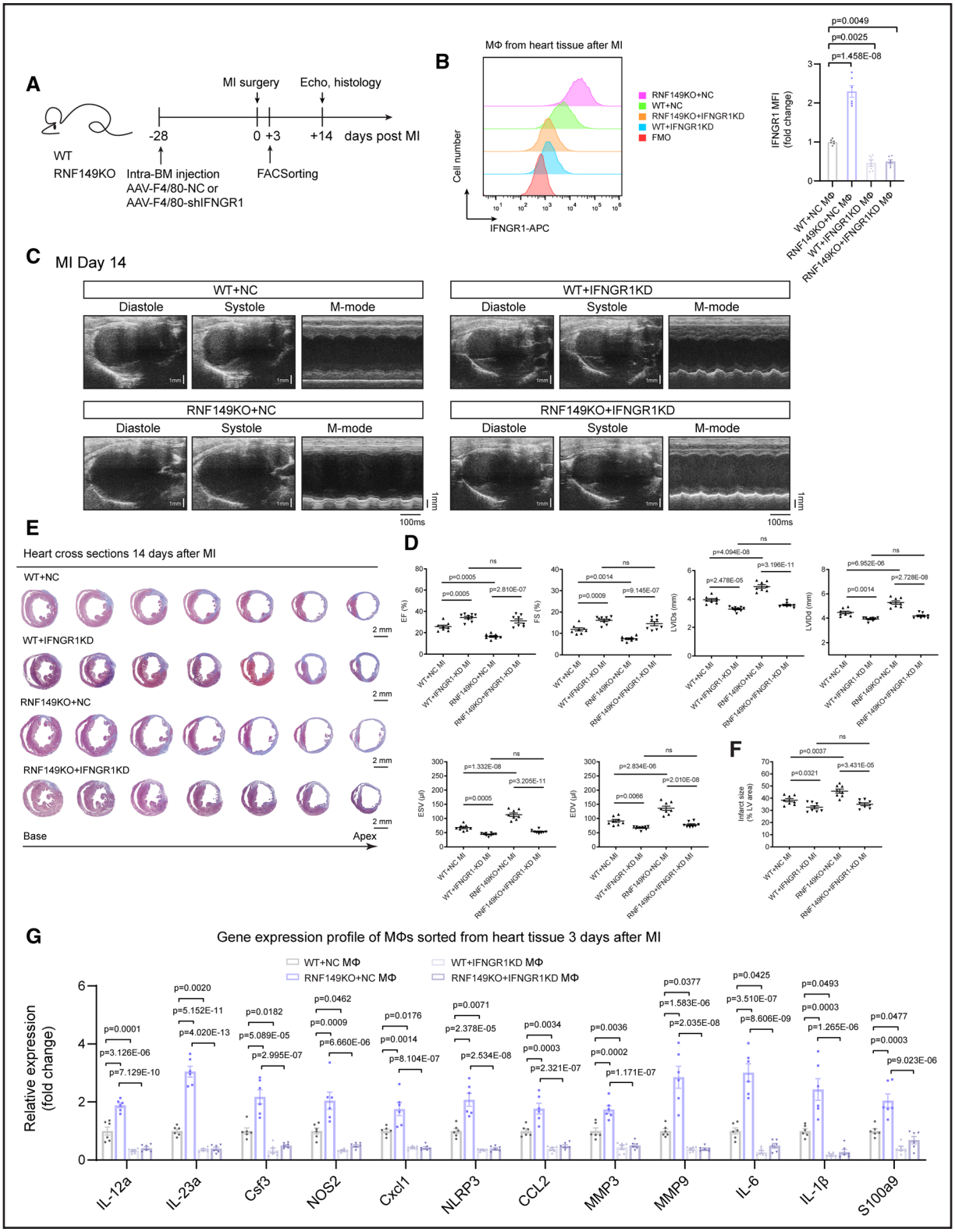

Figure 7. Loss of IFNGR1 (interferon gamma receptor 1) rescues deleterious effects of RNF149 (ring finger protein 149) deficiency on myocardial infarction (MI).

A, Design of the IFNGR1 knockdown (KD) study. **B**, Mean fluorescence intensity (MFI) of IFNGR1 expression on infarct macrophages ($CD45^+CD11b^+Ly6G^-F4/80^+CD64^+$) from the designated groups (n=6). **C**, Wild-type (WT) and RNF149 knockout (RNF149KO) mice were administrated with adeno-associated virus (AAV)-F4/80-shIFNGR1 or AAV-F4/80-NC (nonsense control short hairpin RNA [shRNA]) via intra-bone marrow (BM) injection and, 4 weeks later, were subjected to MI. Representative B-mode and M-mode echocardiograms are shown. **D**, Summarized data of echocardiographic measurements in **C** (n=8, 9, 8, 8). **E**, Representative Masson trichrome staining of heart cross sections from mice of designated groups at day 14 after MI. **F**, Summarized data of infarct size measured from **E** (n=8). **G**, mRNA (*Continued*)

polyubiquitination of endogenous IFNGR1, triggered by IFN-γ treatment, was reduced in *Rnf149*$^{-/-}$ BMDMs compared with *Rnf149*$^{+/+}$ BMDMs (Figure 6F). In summary, these results suggest that RNF149 functions as an E3 ligase for IFNGR1, strongly inducing IFNGR1 ubiquitination and subsequent proteasome-mediated degradation.

Loss of IFNGR1 Rescues the Detrimental Effects of RNF149 Deficiency on MI

To evaluate whether the accumulation of IFNGR1 contributes to the altered macrophage phenotype observed in RNF149-deficient mice following MI, we knocked down IFNGR1 in RNF149KO and WT mice through intra-BM injection of an AAV encoding IFNGR1-short hairpin RNA driven by macrophage-specific F4/80 promoter (AAV-F4/80-shIFNGR1; Figure 7A; Figure S15), as described previously.[14–16] IFNGR1 knockdown in BMDMs and infarct macrophages of AAV-infected mice was confirmed by qPCR and flow cytometry (Figure 7B; Figure S15). Echocardiography showed that IFNGR1 knockdown resulted in elevated ejection fraction and fractional shortening in both WT and RNF149KO mice, whereas decreased end-diastolic volume and LV internal diameter at end diastole. Then, we observed a reduced infarct size in both WT and RNF149KO groups when IFNGR1 was knocked down (Figure 7C and 7F). Furthermore, the upregulation of proinflammatory genes in infarct macrophages caused by RNF149KO was reversed by IFNGR1 knockdown (Figure 7G), supporting the reported phenotypic rescue. Collectively, these results demonstrate that the deleterious effect of RNF149KO on MI depends on the full function of IFNGR1.

Transactivation of *Rnf149* by STAT1 Functions as Negative Feedback Regulation of Type-II IFN Signaling

Through STAT1 ChIP-seq profiling in BMDMs (source data obtained from the GEO data set, GSE84520), we identified STAT1 binding peaks within the *Rnf149* promoter, as illustrated in the genome browser tracks (Figure 8A and 8B). Furthermore, employing the online transcription factor binding sites analysis tool JASPAR, we found 7 evolutionarily conserved STAT1-binding sites within the aforementioned peaks on the *Rnf149* promoter (Figure 8C; Figure S16). Conventional ChIP-qPCR assay in BMDMs confirmed that *Rnf149* promoter fragments containing the putative STAT1-binding sites could be more significantly immunoprecipitated by the STAT1 antibody compared with the anti-IgG antibody (Figure 8C). In addition, IFN-γ stimulation significantly amplified the enrichment of STAT1-bound promoter fragments of *Rnf149* in BMDMs (Figure 8B and 8C). These findings suggest that STAT1 is a transcriptional regulator of *Rnf149* and type-II IFN signaling affects the binding activity of STAT1 to the *Rnf149* promoter. We further investigated whether STAT1 acts as a transcriptional activator for *Rnf149*. Therefore, luciferase reporter constructs driven by the nested deletions of the *Rnf149* promoter were generated and transfected into HEK293T cells (Figure 8D). Luciferase reporter gene activity driven by the *Rnf149* promoter was enhanced by STAT1 overexpression (Figure 8D). These data collectively indicate that type-II IFN signaling orchestrates the transcriptional activation of *Rnf149* through STAT1. These findings align with the observed increase in mRNA and protein levels of *Rnf149* in BMDMs upon IFN-γ stimulation (Figure 8E).

Next, we examined the impact of RNF149 loss on the expression of inflammatory genes in macrophages stimulated with IFN-γ. *Rnf149*$^{-/-}$ BMDMs exhibited a marked upregulation of CD86 upon IFN-γ stimulation (Figure 8F). Additionally, elevated protein levels of pY701-STAT1, along with major inflammatory cytokines, such as IL-6, IL-23 p19, NOS2, and Csf3, were observed in *Rnf149*$^{-/-}$ BMDMs stimulated with IFN-γ (Figure 8G and 8H). Collectively, these in vitro findings support a model that STAT1-mediated transactivation of *Rnf149* serves as negative feedback regulation of type-II IFN signaling in macrophages (Figure S17).

DISCUSSION

Our results identify the role of RNF149 in restraining the proinflammatory state in infarct macrophages and promoting the resolution of inflammation inside the MI hears. Mechanistically, we identify IFNGR1 as a novel RNF149 substrate. Our results demonstrate that RNF149-mediated IFNGR1 ubiquitylation restrains ischemic injury and facilitates cardiac repair by directly controlling macrophage-driven inflammation. We propose that STAT1 activation induces RNF149 transcription, which, in turn, destabilizes the IFNGR1 receptor to counteract type-II IFN signaling and, thereby, inhibits the IFN immune response. Collectively, these findings unveil a heretofore underexplored mechanism that promotes the switch from an inflammatory to a proresolving state in macrophages, contributing to postinfarction cardiac repair.

RNF149, an E3 ligase with a RING domain, has been reported to inhibit the MAPK (mitogen-activated protein kinase) pathway by mediating K48-linked

Figure 7 Continued. levels of major inflammatory genes in infarct macrophages ($CD45^+CD11b^+Ly6G^-F4/80^+CD64^+$) from the designated groups; n=6. Data were analyzed using 2-way ANOVA with the Bonferroni multiple comparisons test (**B**, **D**, **F**, and **G**). CCL2 indicates C-C motif chemokine ligand 2; CD, cluster of differentiation; Csf3, colony stimulating factor 3; Cxcl1, C-X-C motif chemokine ligand 1; FMO, fluorescence minus one; IL, interleukin; MMP, matrix metallopeptidase; MΦ, macrophages; NC, negative control; NLRP3, NOD-, leucine-rich repeats- and pyrin domain-containing protein 3; NOS2, type 2 nitric oxide synthase; ns, not significant; and S100a9, S100 calcium binding protein A9.

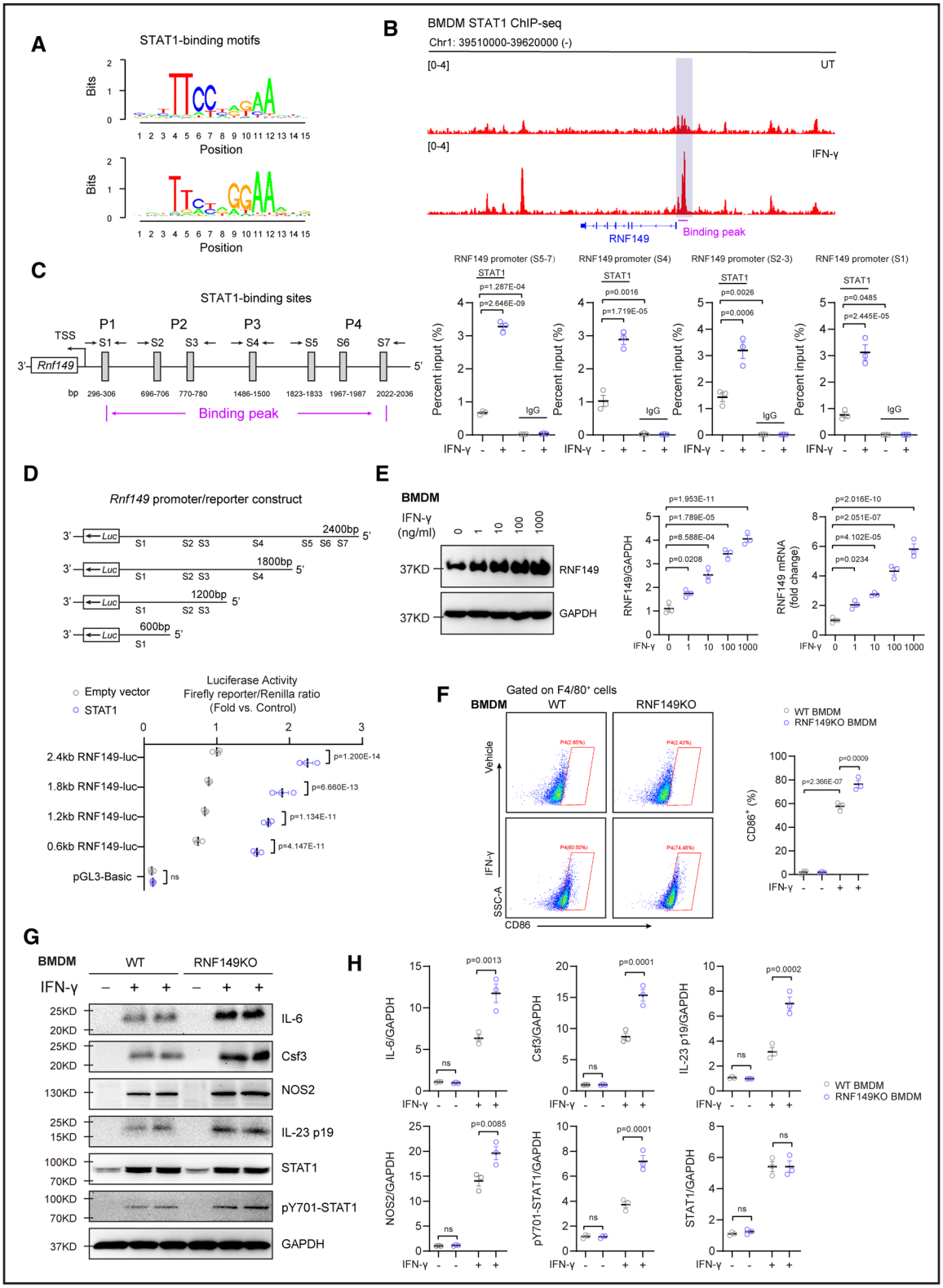

Figure 8. Transactivation of *Rnf149* (ring finger protein 149) by STAT1 (signal transducer and activator of transcription 1) functions as negative feedback regulation of type-II IFN (interferon) signaling.

A, Enriched STAT1-binding motifs (*Z*-score, −23.751; *P*=8.364×10⁻70; calculated by Cistrome SeqPos motif analysis) from STAT1 ChIP-seq in bone marrow–derived macrophages (BMDMs; source data obtained from GEO data set, GSE84520). **B**, STAT1 binding tracks at *Rnf149* gene loci in BMDMs at baseline or after 2 hours of IFN-γ stimulation (raw data retrieved from the GEO data set, GSE84520). The purple line denotes the STAT1-binding peak on the promoter region. **C**, Schematic diagram (**left**) showing conserved STAT1-binding sites within binding peaks on *Rnf149* promoter. The positions of primer pairs (arrowheads) flanking STAT1-binding sites in the *Rnf149* promoter are indicated. ChIP-qPCR (ChIP-quantitative polymerase chain reaction) assay in BMDMs (**right**) for STAT1 or IgG occupancy at *Rnf149* promoter fragments (*Continued*)

polyubiquitination and subsequent proteasomal degradation of BRAF (B-Raf proto-oncogene), a member of the RAF (Raf oncogene) kinase family.[25] This implies the potential involvement of RNF149 in the regulation of diverse cellular activities, including growth, survival, differentiation, and transformation.[25,26] Our studies suggest that RNF149 is a key regulator of macrophage inflammation sensing in the MI tissue. Intriguingly, a multitude of E3 ligases and deubiquitinases, which target protein substrates involved in type-II IFN signaling including the IFN receptor,[24,27] JAKs,[12,24,28,29] and STAT proteins,[30–32] controls an intricate network that finely tunes the inflammatory response. More recently, the linear ubiquitin chain assembly complex (LUBAC) was shown to interact with STAT1, controlling its linear ubiquitination and antiviral IFN signaling.[30] Importantly, RNF149 functions upstream of type-II IFN signaling by specifically binding to IFNGR1 and targeting IFNGR1 for K48-linked polyubiquitination, switching off the inflammatory response. Furthermore, we demonstrate that impaired IFNGR1 degradation, resulting from RNF149 deficiency, augmented STAT1 tyrosine phosphorylation and amplified proinflammatory signals in macrophages. IFNGR1 knockdown rescued excessive inflammation and mitigated the exacerbation of cardiac dysfunction in RNF149-deficient infarcted hearts, indicating IFNGR1 upregulation as the primary mechanism exacerbating post-MI remodeling due to RNF149 loss. Although the aforementioned findings do not completely rule out the involvement of other putative RNF149-binding proteins, they underscore the pivotal role of IFNGR1 as a primary substrate of RNF149 in modulating macrophage inflammation, relegating other substrates to a subordinate role, particularly in the context of MI. Further investigations aimed at validating additional interacting proteins as RNF149 substrates and elucidating their contributions to RNF149KO MI models are warranted to achieve a comprehensive understanding of the underlying mechanisms.

Upon binding of IFN-γ to IFNGR1, JAK1 becomes activated and phosphorylates STAT1 at Tyr701 (tyrosine residue 701). Phosphorylated STAT1 forms homodimers that translocate to the nucleus and bind to GAS (IFN-γ-activated site) elements located in the promoters of certain IFN-γ-regulated genes, such as *CD86*, *IL-23*, and *IL-12*, thereby initiating the transcription of these genes.[21] IFN-γ, a pleiotropic cytokine produced by T cells, natural killer (NK) cells, and macrophages, exhibited a gradual rise in infarcted hearts, contrasting with the early induction of IFNGR1 and pSTAT1 in infarct macrophages after MI. Our findings suggest that RNF149 regulates infiltrating macrophage differentiation by suppressing IFNGR1/STAT1 activation during the acute phase of MI. Thus, the delayed peak of IFN-γ levels implies the presence of additional macrophage-intrinsic inhibitory signaling on IFNGR1/STAT1 during the chronic stage of MI.

IFNGR1 receptors are present in most immune cells. However, we observed upregulation of RNF149 primarily in infarct macrophages, with much lower RNF149 expression in other leukocytes. This observation implies the possible presence of downregulating signaling that may counteract the IFN-γ/STAT1-mediated RNF149 transactivation in other leukocyte populations within infarcted myocardium. Increased cell-surface IFNGR1 expression level has been demonstrated to augment the responsiveness to IFN-γ signaling.[23,24] Our data demonstrate that as a result of IFNGR1 stabilization, RNF149 loss amplified inflammatory cytokine expression in macrophages in response to IFN-γ. Here, we elucidate the cell-autonomous regulation of IFNGR1 itself. As a type-II IFN signaling–induced E3 ligase, RNF149 orchestrates the proteasomal degradation of its core component, IFNGR1, akin to the known feedback control mechanism mediated by the suppressor of cytokine signaling.[29] Interestingly, this ubiquitination-mediated control of IFNGR1 stability appears to represent a common regulatory mechanism, as recent studies have implicated 2 other ubiquitin ligases, STUB1 (stress-induced phosphoprotein 1 homology and U-box containing protein 1) and FBXW7 (F-box and WD repeat domain containing 7), in governing IFNGR1 signaling in tumor cells.[23,24,33] Our findings complement these studies and underscore the importance of ubiquitin-mediated IFNGR1 modulation.

Sustained inflammatory response and failure of inflammation resolution are associated with maladaptive cardiac remodeling after MI.[34] The timely resolution of inflammation is crucial for effective cardiac repair postischemic injury.[4] The feedback loop involving STAT1-mediated RNF149 transactivation and the subsequent destabilization of IFNGR1 offers a mechanism to dampen type-II IFN response in macrophages, thereby preventing excessive inflammation. Infarct macrophages influence

Figure 8 Continued. containing STAT1-binding sites (n=3). **D**, Generation of luciferase reporters controlled by *Rnf149* promoter or truncated mutants (**top**); *Rnf149* transcriptional activity assay in HEK293T cells cotransfected with luciferase reporter driven by indicated promoter and pRL-TK-renilla, along with expression plasmid for STAT1 or empty vector (EV; **bottom**). n=3 independent batches of experiments and 3 transfection replications for each batch. **E**, Dose dependence of IFN-γ stimulation on RNF149 expression in BMDMs (n=3). **F**, Representative flow cytometry profiles and quantification of $CD86^+$ (%) in $Rnf149^{+/+}$ or $Rnf149^{-/-}$ BMDMs stimulated with vehicle or IFN-γ (n=3). **G**, Immunoblot analysis of the expression level of STAT1, pY701-STAT1, and inflammatory cytokines in $Rnf149^{+/+}$ or $Rnf149^{-/-}$ BMDMs incubated with or without IFN-γ. **H**, Quantification of G (n=3). Data were analyzed using 2-way ANOVA with the Bonferroni multiple comparisons test (**C**, **D**, **F**, and **H**) and 1-way ANOVA with the Dunnett multiple comparisons test (**E**). CD indicates cluster of differentiation; ChIP-qPCR, chromatin immunoprecipitation quantitative polymerase chain reaction; Csf3, colony stimulating factor 3; IL, interleukin; NOS2, type 2 nitric oxide synthase; pRL-TK, thymidine kinase promoter-Renilla luciferase reporter plasmid; pY701, phosphorylation at tyrosine 701; STAT, signal transducer and activator of transcription; TSS, transcription start site; and UT, no treatment.

neighboring cardiac cells through paracrine cytokine signaling.[2] RNF149-deficient infarct macrophages exhibited heightened expression of IL-6, IL-23a, Csf3, and MMP9, which are recognized mediators of inflammatory myocardial injury and adverse remodeling post-MI.[2,6,8,19] MMP9, an extracellular matrix-degrading enzyme, has been shown to degrade collagens and impede infarct repair.[6,8,35] Conversely, RNF149KO infarct macrophages displayed reduced expression of VEGF-α and TGF-β, which are known for their roles in promoting angiogenesis and α-SMA$^+$ myofibroblast proliferation post-MI, respectively.[2,4,36] The impairment of myofibroblast proliferation, angiogenesis, and collagen I deposition in the IA contributes to the formation of reparative granulation tissue with reduced collagen density, fewer stress fibers, and diminished tensile strength, ultimately insufficient to sustain structural integrity and suppress infarct expansion.[4,6] Therefore, RNF149KO mice exhibited larger infarct size and exacerbated heart dysfunction after MI, attributed to increased cardiac injury and impaired infarct repair, as evidenced by elevated myocardial apoptosis and the formation of collagen-scarce scar. In line with these findings, our bulk transcriptome data revealed marked upregulation of multiple genes associated with the amplification of inflammatory response and the recruitment of mobilized leukocytes in RNF149KO infarcts. Therefore, RNF149 holds profound significance in regulating the intensity and duration of inflammatory signaling in macrophages. This regulatory mechanism assumes a pivotal role in fine-tuning the immune response and preserving immune homeostasis in the aftermath of MI.

The current understanding of cardiac macrophage subsets and their roles in MI is gradually expanding.[2,3] In the early stages of MI, monocyte-derived CCR2$^+$ macrophages exhibit proinflammatory characteristics and have been implicated in the promotion of adverse remodeling.[2,3] In this study, we show that RNF149 was mainly expressed in CCR2$^+$MHC-II^{high} cardiac macrophages in MI mice. RNF149 demonstrates a predominant role in modulating proinflammatory signaling in infarct macrophages, as substantiated by the observation that RNF149 loss had a more pronounced impact on the expression of proinflammatory genes in infarct macrophages compared with those genes associated with reparative functions. Further analysis of macrophage subsets confirms these findings. The excessive infiltration of proinflammatory monocyte/macrophage populations due to RNF149 loss contributes to the maintenance of a high-intensity inflammatory microenvironment within the infarcted myocardium, which, in turn, hinders the formation of reparative macrophage subset, culminating in myocardial injury, suboptimal infarct repair, and maladaptive remodeling following MI.

Our present study primarily investigates the role and mechanism of RNF149 in cardiac repair, along with an early intervention strategy targeting RNF149 in a murine MI model. Notably, we observed an accumulation of RNF149$^+$ macrophages in heart tissue samples from patients with MI. Recent studies have highlighted the therapeutic potential of proresolving agents in addressing uncontrolled inflammation.[37] However, no RNF149 agonists have been identified to date. Ad represents a gene therapy tool employing modified adenoviruses as vehicles for therapeutic gene delivery to cardiac cells.[38] Transient overexpression of RNF149 in infarct macrophages early after MI via Ad-mediated gene transfer has shown efficacy in improving cardiac function in murine MI models. The massive occlusion of coronary artery blood supply in the IA, especially in the early stage of MI, impedes the accumulation of therapeutic agents administered via intravenous injection.[38] Despite the invasiveness of intramyocardial injection, it provides a direct route for Ad delivery to the infarcted myocardium. Furthermore, adenoviral gene transfer via percutaneous intracoronary administration offers a practical, reproducible, and safe approach for treating myocardial ischemia.[39,40] It is tempting to hypothesize that engineered adenoviruses encoding RNF149 under a macrophage-specific promoter or nanoparticles containing RNF149 mRNA could be delivered to the infarcted hearts through intracoronary injection during reperfusion therapy for patients with acute MI.

In summary, our mechanistic and functional data position RNF149 as a critical determinant of inflammatory signaling in infarct macrophages through its destabilizing effects on IFNGR1, thereby restraining myocardial inflammatory response and promoting infarct healing post-MI. Our findings contribute novel insights into mechanisms governing post-MI inflammation balance. Consequently, targeting macrophage RNF149 may represent an innovative and promising therapeutic strategy to treat MI.

ARTICLE INFORMATION

Received November 20, 2023; revision received July 1, 2024; accepted July 2, 2024.

Affiliations

Cardiovascular Department, First Affiliated Hospital, Fujian Medical University, Fuzhou, Fujian, China (C.-K.H., Z.Z., S.C., L.C., D.C.). Department of Cardiovascular Medicine, Ruijin Hospital, Shanghai Jiao Tong University School of Medicine, Shanghai, China (C.-K.H., Z.C., X.Y.). Department of Forensic Medicine, School of Basic Medical Sciences, Fudan University, Shanghai, China (L.L.). Department of Anesthesiology, Laboratory of Mitochondrial Metabolism and Perioperative Medicine, West China Hospital, Sichuan University, Chengdu, Sichuan, China (T.L.).

Sources of Funding

This study was supported by the National Natural Science Foundation of China (grant 82100522 to C.-K. Huang) and the Fujian Provincial Health Technology Project (grant 2023GGA025 to C.-K. Huang and grant 2021ZQNZD005 to D. Chai).

Disclosures

None.

Supplemental Material

Extended Methods
Figures S1–17
Tables S1–11

REFERENCES

1. Tsao CW, Aday AW, Almarzooq ZI, Anderson CAM, Arora P, Avery CL, Baker-Smith CM, Beaton AZ, Boehme AK, Buxton AE, et al; American Heart Association Council on Epidemiology and Prevention Statistics Committee and Stroke Statistics Subcommittee. Heart disease and stroke statistics-2023 update: a report from the American Heart Association. *Circulation*. 2023;147:e93–e621. doi: 10.1161/CIR.0000000000001123
2. Yap J, Irei J, Lozano-Gerona J, Vanapruks S, Bishop T, Boisvert WA. Macrophages in cardiac remodelling after myocardial infarction. *Nat Rev Cardiol*. 2023;20:373–385. doi: 10.1038/s41569-022-00823-5
3. Kubota A, Frangogiannis NG. Macrophages in myocardial infarction. *Am J Physiol Cell Physiol*. 2022;323:C1304–C1324. doi: 10.1152/ajpcell.00230.2022
4. Prabhu SD, Frangogiannis NG. The biological basis for cardiac repair after myocardial infarction: from inflammation to fibrosis. *Circ Res*. 2016;119:91–112. doi: 10.1161/CIRCRESAHA.116.303577
5. Fan Q, Tao R, Zhang H, Xie H, Lu L, Wang T, Su M, Hu J, Zhang Q, Chen Q, et al. Dectin-1 contributes to myocardial ischemia/reperfusion injury by regulating macrophage polarization and neutrophil infiltration. *Circulation*. 2019;139:663–678. doi: 10.1161/CIRCULATIONAHA.118.036044
6. Huang CK, Dai D, Xie H, Zhu Z, Hu J, Su M, Liu M, Lu L, Shen W, Ning G, et al. Lgr4 governs a pro-inflammatory program in macrophages to antagonize post-infarction cardiac repair. *Circ Res*. 2020;127:953–973. doi: 10.1161/CIRCRESAHA.119.315807
7. Yan X, Anzai A, Katsumata Y, Matsuhashi T, Ito K, Endo J, Yamamoto T, Takeshima A, Shinmura K, Shen W, et al. Temporal dynamics of cardiac immune cell accumulation following acute myocardial infarction. *J Mol Cell Cardiol*. 2013;62:24–35. doi: 10.1016/j.yjmcc.2013.04.023
8. Yan X, Zhang H, Fan Q, Hu J, Tao R, Chen Q, Iwakura Y, Shen W, Lu L, Zhang Q, et al. Dectin-2 deficiency modulates Th1 differentiation and improves wound healing after myocardial infarction. *Circ Res*. 2017;120:1116–1129. doi: 10.1161/CIRCRESAHA.116.310260
9. Andreadou I, Cabrera-Fuentes HA, Devaux Y, Frangogiannis NG, Frantz S, Guzik T, Liehn EA, Gomes CPC, Schulz R, Hausenloy DJ. Immune cells as targets for cardioprotection: new players and novel therapeutic opportunities. *Cardiovasc Res*. 2019;115:1117–1130. doi: 10.1093/cvr/cvz050
10. Hu H, Sun SC. Ubiquitin signaling in immune responses. *Cell Res*. 2016;26:457–483. doi: 10.1038/cr.2016.40
11. Jiang X, Chen ZJ. The role of ubiquitylation in immune defence and pathogen evasion. *Nat Rev Immunol*. 2011;12:35–48. doi: 10.1038/nri3111
12. Liu YC, Penninger J, Karin M. Immunity by ubiquitylation: a reversible process of modification. *Nat Rev Immunol*. 2005;5:941–952. doi: 10.1038/nri1731
13. Guillamot M, Ouazia D, Dolgalev I, Yeung ST, Kourtis N, Dai Y, Corrigan K, Zea-Redondo L, Saraf A, Florens L, et al. The E3 ubiquitin ligase SPOP controls resolution of systemic inflammation by triggering MYD88 degradation. *Nat Immunol*. 2019;20:1196–1207. doi: 10.1038/s41590-019-0454-6
14. Fellmann C, Hoffmann T, Sridhar V, Hopfgartner B, Muhar M, Roth M, Lai DY, Barbosa IA, Kwon JS, Guan Y, et al. An optimized microRNA backbone for effective single-copy RNAi. *Cell Rep*. 2013;5:1704–1713. doi: 10.1016/j.celrep.2013.11.020
15. Zhao HY, Zhang YY, Xing T, Tang SQ, Wen Q, Lyu ZS, Lv M, Wang Y, Xu LP, Zhang XH, et al. M2 macrophages, but not M1 macrophages, support megakaryopoiesis by upregulating PI3K-AKT pathway activity. *Signal Transduct Target Ther*. 2021;6:234. doi: 10.1038/s41392-021-00627-y
16. Xiao Z, Wei X, Li M, Yang K, Chen R, Su Y, Yu Z, Liang Y, Ge J. Myeloid-specific deletion of Capns1 attenuates myocardial infarction injury via restoring mitochondrial function and inhibiting inflammasome activation. *J Mol Cell Cardiol*. 2023;183:54–66. doi: 10.1016/j.yjmcc.2023.08.006
17. Mathiyalagan P, Adamiak M, Mayourian J, Sassi Y, Liang Y, Agarwal N, Jha D, Zhang S, Kohlbrenner E, Chepurko E, et al. FTO-dependent N(6)-methyladenosine regulates cardiac function during remodeling and repair. *Circulation*.2019;139:518–532.doi:10.1161/CIRCULATIONAHA.118.033794
18. Jia D, Chen S, Bai P, Luo C, Liu J, Sun A, Ge J. Cardiac resident macrophage-derived legumain improves cardiac repair by promoting clearance and degradation of apoptotic cardiomyocytes after myocardial infarction. *Circulation*. 2022;145:1542–1556. doi: 10.1161/CIRCULATIONAHA.121.057549
19. Frangogiannis NG. The inflammatory response in myocardial injury, repair, and remodelling. *Nat Rev Cardiol*. 2014;11:255–265. doi: 10.1038/nrcardio.2014.28
20. Huang da W, Sherman BT, Lempicki RA. Systematic and integrative analysis of large gene lists using DAVID bioinformatics resources. *Nat Protocols*. 2009;4:44–57. doi: 10.1038/nprot.2008.211
21. Schneider WM, Chevillotte MD, Rice CM. Interferon-stimulated genes: a complex web of host defenses. *Annu Rev Immunol*. 2014;32:513–545. doi: 10.1146/annurev-immunol-032713-120231
22. Deshaies RJ, Joazeiro CA. RING domain E3 ubiquitin ligases. *Annu Rev Biochem*. 2009;78:399–434. doi: 10.1146/annurev.biochem.78.101807.093809
23. Londino JD, Gulick DL, Lear TB, Suber TL, Weathington NM, Masa LS, Chen BB, Mallampalli RK. Post-translational modification of the interferon-gamma receptor alters its stability and signaling. *Biochem J*. 2017;474:3543–3557. doi: 10.1042/BCJ20170548
24. Apriamashvili G, Vredevoogd DW, Krijgsman O, Bleijerveld OB, Ligtenberg MA, de Bruijn B, Boshuizen J, Traets JJH, D'Empaire Altimari D, van Vliet A, et al. Ubiquitin ligase STUB1 destabilizes IFNγ-receptor complex to suppress tumor IFNγ signaling. *Nat Commun*. 2022;13:1923. doi: 10.1038/s41467-022-29442-x
25. Hong SW, Jin DH, Shin JS, Moon JH, Na YS, Jung KA, Kim SM, Kim JC, Kim KP, Hong YS, et al. Ring finger protein 149 is an E3 ubiquitin ligase active on wild-type v-Raf murine sarcoma viral oncogene homolog B1 (BRAF). *J Biol Chem*. 2012;287:24017–24025. doi: 10.1074/jbc.M111.319822
26. Wu X, Wu Z, Deng W, Xu R, Ban C, Sun X, Zhao Q. Spatiotemporal evolution of AML immune microenvironment remodeling and RNF149-driven drug resistance through single-cell multidimensional analysis. *J Transl Med*. 2023;21:760. doi: 10.1186/s12967-023-04579-5
27. Henrich IC, Jain K, Young R, Quick L, Lindsay JM, Park DH, Oliveira AM, Blobel GA, Chou MM. Ubiquitin-specific protease 6 functions as a tumor suppressor in Ewing sarcoma through immune activation. *Cancer Res*. 2021;81:2171–2183. doi: 10.1158/0008-5472.CAN-20-1458
28. Kim H, Frederick DT, Levesque MP, Cooper ZA, Feng Y, Krepler C, Brill L, Samuels Y, Hayward NK, Perlina A, et al. Downregulation of the ubiquitin ligase RNF125 underlies resistance of melanoma cells to BRAF inhibitors via JAK1 deregulation. *Cell Rep*. 2015;11:1458–1473. doi: 10.1016/j.celrep.2015.04.049
29. Kile BT, Alexander WS. The suppressors of cytokine signalling (SOCS). *Cell Mol Life Sci*. 2001;58:1627–1635. doi: 10.1007/PL00000801
30. Zuo Y, Feng Q, Jin L, Huang F, Miao Y, Liu J, Xu Y, Chen X, Zhang H, Guo T, et al. Regulation of the linear ubiquitination of STAT1 controls antiviral interferon signaling. *Nat Commun*. 2020;11:1146. doi: 10.1038/s41467-020-14948-z
31. Perng YC, Lenschow DJ. ISG15 in antiviral immunity and beyond. *Nat Rev Microbiol*. 2018;16:423–439. doi: 10.1038/s41579-018-0020-5
32. Guo X, Ma P, Li Y, Yang Y, Wang C, Xu T, Wang H, Li C, Mao B, Qi X. RNF220 mediates K63-linked polyubiquitination of STAT1 and promotes host defense. *Cell Death Differ*. 2021;28:640–656. doi: 10.1038/s41418-020-00609-7
33. Singh S, Kumar S, Srivastava RK, Nandi A, Thacker G, Murali H, Kim S, Baldeon M, Tobias J, Blanco MA, et al. Loss of ELF5-FBXW7 stabilizes IFNGR1 to promote the growth and metastasis of triple-negative breast cancer through interferon-γ signalling. *Nat Cell Biol*. 2020;22:591–602. doi: 10.1038/s41556-020-0495-y
34. Swirski FK, Nahrendorf M. Cardioimmunology: the immune system in cardiac homeostasis and disease. *Nat Rev Immunol*. 2018;18:733–744. doi: 10.1038/s41577-018-0065-8
35. Seropian IM, Toldo S, Van Tassell BW, Abbate A. Anti-inflammatory strategies for ventricular remodeling following ST-segment elevation acute myocardial infarction. *J Am Coll Cardiol*. 2014;63:1593–1603. doi: 10.1016/j.jacc.2014.01.014
36. Howangyin KY, Zlatanova I, Pinto C, Ngkelo A, Cochain C, Rouanet M, Vilar J, Lemitre M, Stockmann C, Fleischmann BK, et al. Myeloid-epithelial-reproductive receptor tyrosine kinase and milk fat globule epidermal growth factor 8 coordinately improve remodeling after myocardial infarction via local delivery of vascular endothelial growth factor. *Circulation*. 2016;133:826–839. doi: 10.1161/CIRCULATIONAHA.115.020857
37. Serhan CN, Levy BD. Resolvins in inflammation: emergence of the pro-resolving superfamily of mediators. *J Clin Invest*. 2018;128:2657–2669. doi: 10.1172/JCI97943
38. Yang Q, Fang J, Lei Z, Sluijter JPG, Schiffelers R. Repairing the heart: state-of-the-art delivery strategies for biological therapeutics. *Adv Drug Deliv Rev*. 2020;160:1–18. doi: 10.1016/j.addr.2020.10.003
39. Hedman M, Hartikainen J, Syvänne M, Stjernvall J, Hedman A, Kivelä A, Vanninen E, Mussalo H, Kauppila E, Simula S, et al. Safety and feasibility of catheter-based local intracoronary vascular endothelial growth factor gene transfer in the prevention of postangioplasty and in-stent restenosis and in the treatment of chronic myocardial ischemia: phase II results of the Kuopio Angiogenesis Trial (KAT). *Circulation*. 2003;107:2677–2683. doi: 10.1161/01.CIR.0000070540.80780.92
40. Grines CL, Watkins MW, Mahmarian JJ, Iskandrian AE, Rade JJ, Marrott P, Pratt C, Kleiman N; Angiogene GENe Therapy (AGENT-2) Study Group. A randomized, double-blind, placebo-controlled trial of Ad5FGF-4 gene therapy and its effect on myocardial perfusion in patients with stable angina. *J Am Coll Cardiol*. 2003;42:1339–1347. doi: 10.1016/s0735-1097(03)00988-4